SEQUENCE STRATIGRAPHY AND DETRITAL ZIRCON GEOCHRONOLOGY OF MIDDLE-LATE ORDOVICIAN MT. WILSON QUARTZITE, BRITISH COLUMBIA CANADA

A Thesis

by

ANDREW PAUL HUTTO

Submitted to the Office of Graduate Studies of
Texas A&M University
in partial fulfillment of the requirements for the degree of

MASTER OF SCIENCE

May 2012

Major Subject: Geology

Sequence Stratigraphy and Detrital Zircon Geochronology of Middle-Late Ordovician Mt. Wilson Quartzite, British Columbia, Canada

SEQUENCE STRATIGRAPHY AND DETRITAL ZIRCON GEOCHRONOLOGY OF MIDDLE -LATE ORDOVICIAN MT. WILSON QUARTZITE, BRITISH COLUMBIA, CANADA

A Thesis

by

ANDREW PAUL HUTTO

Submitted to the Office of Graduate Studies of
Texas A&M University
in partial fulfillment of the requirements for the degree of

MASTER OF SCIENCE

Approved by:

Chair of Committee,	Michael C. Pope
Committee Members,	Walter B. Ayers
	Brent V. Miller
Head of Department,	John R. Giardino

May 2012

Major Subject: Geology

ABSTRACT

Sequence Stratigraphy and Detrital Zircon Geochronology of Middle-Late Ordovician Mt. Wilson Quartzite, British Columbia, Canada. (May 2012)

Andrew Paul Hutto, B.S. Geology, Texas A&M University

Chair of Advisory Committee: Dr. Michael Pope

The Middle-Late Ordovician Mt. Wilson Quartzite, southern British Columbia, Canada, is a supermature quartz arenite deposited in shallow marine-marginal marine environments on the Early Paleozoic western Laurentian passive margin. Facies-stacking patterns indicate the Mt. Wilson Quartzite is an unconformity bounded, 2nd-order depositional sequence, containing two 3rd-order sequences, and numerous parasequences.

Detrital zircon age spectra of six samples of the Mt. Wilson Quartzite have numerous peaks that are unique to Middle to Late Ordovician quartz arenites of western Laurentia. The main peaks, 1800-2000 Ma, 2000-2200 Ma, and 2300-2400 Ma are interpreted to have been derived from basement rocks that were exposed east of the study area: Trans-Hudson Orogeny (1800-2000 Ma), Taltson Orogen (1800-2000 Ma), Buffalo Head Terrane (2000-2400 Ma), Paleoproterozoic crust (2000-2400 Ma), and the Wopmay Terrane (2000-2400 Ma). It is likely that these areas were sourced by local rivers and tributaries draining the Transcontinental Arch and delivered sediment to the deposition location of the Mt. Wilson Quartzite. While longshore transport was a viable

distribution method for sediment along the passive margin, it is unlikely that the Peace River Arch (located northwest of the Mt. Wilson Quartzite) was its sole point source; rather it is more likely that there were multiple sediment sources for these western Laurentian quartz arenites. Temporal changes in provenance indicate different areas of basement rock were exposed throughout the deposition of the Mt. Wilson Quartzite, most likely reflecting long-term flooding of North America. The potential for spatial changes in provenance remains unsolved.

ACKNOWLEDGEMENTS

I would like to thank my committee chair, Dr. Pope, and my committee members, Dr. Miller and Dr. Ayers, for their guidance and support throughout the course of this research.

Thanks also go to my friends and colleagues and the department faculty and staff for making my time at Texas A&M University a great experience. I also want to extend my gratitude to the Geological Society of America, through which I received a grant that helped in the completion of the field study portion of this thesis.

Finally, thanks to my wife for her continued patience and love, and, my family for their support and relentless encouragement.

TABLE OF CONTENTS

LIST OF FIGURES

LIST OF TABLES

Page

1. INTRODUCTION

The Middle-Late Ordovician Mt. Wilson Quartzite, southern British Columbia, Canada, is a supermature quartz arenite deposited on the Early Paleozoic passive margin (Figure 1) of western Laurentia. Similar, coeval quartz arenites (Kinnikinic, Swan Peak, Eureka, etc.) were deposited throughout the US Cordillera and into northern Mexico (Figure 2). These units generally range in thickness from 50 – 150 m and were deposited within a kilometers-thick carbonate dominated platform succession. Depositional environments for these units range from non-marine to nearshore and shallow marine settings; which interfinger with, and grade into shale and carbonate in deeper water environments (Webb, 1958). While much of these units were deposited during a prolonged Middle Ordovician sea level lowstand (Webb, 1958), recent biostratigraphic data indicates that some of these quartz arenites are Cincinnatian (Sweet, 2000), deposited during the most extensive continental flooding of the Paleozoic (Algeo and Seslavinsky, 1995). Decreased grain size and increased sorting (Ketner, 1968), and detrital zircon populations (Gehrels and Dickinson, 1995) were suggested to indicated that the source area for these sediments was the Peace River Arch, Canada and longshore transport moved them to their current location (Gehrels et al., 1995). This suggests there was a proximal point source for the Mt. Wilson Quartzite.

Previous work on the Mt Wilson Quartzite described this unit as massive and featureless (Norford, 1969). This paper presents a detailed sequence stratigraphic framework for the Middle-Late Ordovician Mt. Wilson Quartzite, British Columbia,

---

This thesis follows the style of *Canadian Journal of Earth Science.*

Canada, to outline its record of long-term sea level change. Detrital zircon geochronology of this unit is integrated into the sequence stratigraphic framework to determine the provenance of these sediments.

1.1 Geologic Background

Laurentia formed through collision and amalgamation of continental fragments and arcs throughout the Proterozoic (Hoffman, 1992). The creation and break-up of the supercontinent Rodinia was integral in the formation of Laurentia, providing a central craton core that is surrounded on all sides by Early Paleozoic passive margins (Whitmeyer and Karlstrom, 2007). The central part of the North American continent is stable, covered by generally flat-lying sediment, however, the western portion is consists of basement rocks associated with orogenic and accretionary events, both inboard and outboard of the formation of Laurentia (Irving and McGlynn, 1976; Hammer, 2011). The basement terranes of Western Canada are of particular interest for this thesis because they likely provided the sediment to form the Mt. Wilson Quartz arenite and other siliciclastic sedimentary bodies in the region.

The Late Ordovician Mt. Wilson Quartzite (Figure 3) was deposited unconformably above the Middle Ordovician Owen Creek Formation (mostly dolostone) or Glenogle Shale and is unconformably overlain by the Late Ordovician Beaverfoot Formation (limestone and dolostone; Norford, 1969). The nature of the lower contact in most cases is sharp whereas the upper contact is sharp, but rarely visible. Post-depositional orogenic activity, associated with the Cordilleran orogeny, began around 250 Ma (Miall and Blakey, 2008) and led to intense deformation near the study area. Thus, beds of the Mt.

Wilson are now either steeply dipping or completely overturned and contained within several adjacent thrust sheets (Price, 1994), making physical correlation between sections difficult.

Previously, the Mt. Wilson quartz arenite was described in terms of lithostratigraphy, (i.e. correlating lithologies) as being massive and mostly featureless, with a general absence of visible bedding, biologic activity, and poorly defined laminae and sedimentary structures (Norford, 1969). However, these structures were recognized in this study and are described here in detail for multiple sections of the Mt. Wilson quartzite.

Early provenance work suggested that the Peace River Arch was the main source area for the Mt. Wilson Quartzite and related units further south (Ketner, 1968). Longshore transport was invoked to explain the transport of these sediments with the Peace River Arch being a point source. Previous zircon provenance studies indicated that the Peace River Arch was the sole provenance area of the Middle-Late Ordovician quartz arenites (Gehrels et al., 1995; Gehrels, 2000).

The depositional pattern observed in this study, a siliciclastic section between two thick carbonate sequences, occurs in many Middle-Late Ordovician successions surrounding the Transcontinental Arch, making the study of the Mt. Wilson Quartzite important to the understanding of Middle-Late Ordovician sediment transport systems in western Laurentia. This sequence stratigraphic study provides a better framework for understanding the depositional processes for supermature siliciclastic sediments. Both eustasy and tectonism can influence marginal marine deposits; however, provenance

variations of this unit reflect mainly long-term eustatic processes. Understanding how eustasy affected the depositional processes and provenance of these rocks may help our understanding of the deposition of other supermature siliciclastic units.

2. METHODS

Detailed fieldwork included measuring four sections (30 to 250 m thick) of the Mt. Wilson quartz arenite with a Jacob's staff and subdividing individual beds that ranged from 10 cm to more than 1.5 m thick (Figure 3). Horizons of stratigraphic importance were chosen based on distinct changes in lithology, bioturbation, bedding or stratigraphic position. Samples (~5 kg) for detrital zircon analysis were collected from fresh surfaces with a sledge hammer that was cleaned with a wire brush between each sampling. Six samples were analyzed from three measured sections. The Morberley Mountain section has three samples (top, bottom, and middle); the Kicking Horse Canyon section has two samples (top and bottom). Only the top of the Pedley Pass Section was analyzed because it is so much thinner (< 30 m). The Wilcox Pass section was only measured and had no samples analyzed. These sections are correlated based on available biostratigraphy (Cecile and Norford, 1991; L. Pyle, personal communication, 2011).

Sequence stratigraphic analysis of the measured sections was completed using techniques described in earlier siliciclastic studies (e.g., Mitchum and Van Wagoner, 1991; Catuneanu, 2006); including: 1) identifying the depositional environment of the different facies in the measured sections; 2) identifying patterns in the stacking of these facies; 3) interpreting where the important surfaces occur; and, 4) correlating the different sections based on sediment filling available accommodation space.

Zircon separation processes included hammering the rocks into smaller pieces followed by standard crushing and disc milling techniques. A Wilfley table with a peak

angle of 30˚ was used to separate heavier minerals, including detrital zircon grains, from lighter grains. A neodymium-boron magnetic separation removed magnetic minerals and metal fragments from the disc milling. This was followed by heavy liquid (MEI) separation, after which the samples were examined under microscope and zircon grains were separated from other minerals. The zircon grains and standards (FC-1 and Peixe) were then mounted in 1" diameter epoxy resin pucks. The pucks were polished using 6 μm, 1 μm, and 0.25 μm diamond polishing disks, and they were then carbon coated. The pucks were scanned and imaged at Texas A&M University using a Cameca SVX50 microprobe that generated back-scattered electron (BSE) and cathodoluminescence (CL) images of each of the six samples. The images aided in determining the best location to analyze on each grain and which grains to avoid due to internal zoning.

Two main strategies are used in detrital zircon analysis (Fedo et al., 2003). One method is a qualitative analysis in which ages representing source components within individual zircon populations are sought. The advantage of this method is that it may capture age components that a random selection may miss (Gehrels, 2000). Typically, TIMS and Secondary Ionization Mass Spectrometry (SIMS) detrital zircon analyses are used in this strategy (Fedo et al., 2003). This approach was used to establish a reference data set for the western Laurentian Middle-Late Ordovician quartz arenites (Gehrels et al., 1995; Gehrels, 2000).

A second strategy is a quantitative analysis, that allows for the resultant data to be as representative of the total zircon population as possible through spot analysis of many different grains. Analyses with relatively higher accuracy are weighted more. However,

data biasing can be a problem, and minimizing handling of samples may enhance the randomness of grain selection during preparation (Fedo et al., 2003). To limit biasing, the zircon grains in this analysis were scooped en-mass from a petri-dish and subsequently mounted in epoxy resin. In analyzing the mounted zircons, the only operator input was avoiding any zircons with obvious zoning and/or metamict zones. There are sources for bias from the beginning of this process and it is important to be exact in the steps followed to attain zircon samples.

For a sample to be representative of the overall zircon population, the sample size must be statistically adequate. According to statistical analysis, between 60 and 117 grains must be analyzed for the resultant data to be statistically adequate (Dodson et al. 1988; Vermeesch, 2004). The latter strategy allows for this number of grain analyses to be achieved in a time and cost effective way. TIMS analysis of these same zircon populations could provide further insight in the provenance investigation. The grains in this study were analyzed by laser ablation-inductively coupled plasma mass spectrometry (LA-ICPMS) at Washington State University (WSU). Data analysis and collection followed methods of Chang et al. (2006). More than 100 grains in each sample were analyzed for a total sample size of >600 grains from the six samples. The laser was operated at 75-80% power at 5 Hz with a laser width of 30 μm. The quantitative analysis enables comparisons between the proportions of age components of each sample (Fedo et al., 2003).

Data were reduced using standard statistical methods, and then the data were plotted using Isoplot 3.00 (Ludwig, 2003). The data are presented in two graphs: the binned

histogram and the probability density diagram. The binned histogram has two critical limitations (Fedo et al., 2003; Sircombe, 2000; and Vermeesch, 2004). The first limitation is that the associated errors of each analysis are not included in the numerical count for the histogram. The second limitation is that bin widths are arbitrary, and a minor change to bin widths can cause the histogram to have a drastically different appearance. Bin widths vary in literature ranging from 5 Ma (Davis et al., 1994) through 20 Ma (Gehrels and Dickinson, 1995), 33.3 Ma (Scott and Gauthier, 1996), up to 100 Ma (Roback and Walker, 1995). The bin widths in this study are 50 Ma.

The probability density diagram, another common method for displaying detrital zircon geochronology data (Sircombe, 2000), takes into account individual age errors in calculating the probability density distribution. This eliminates the potential for altering the appearance of the diagram by changing the bin widths. However, a limitation of probability density diagram is that the curve cannot be easily read for actual number of grains (Sircombe, 2000). The area beneath the curve conveys frequency and proportion information, such that the height on probability density diagrams is not related just to the total number of analyses in a specific age range, but also to the precision of the data within a specific age range (Sircombe, 2000). To combat the limitations of both methods, a display combining the two is typically used to efficiently display the data (Fedo et al., 2003; Sircombe, 2000; and Vermeesch, 2004). The data from this study (Figure 7) were plotted by both means to facilitate correlation between these and previously published data.

3. RESULTS

The results of this study are presented in three parts. First, the measured sections are correlated in a north-south cross-section. Second, a description of the facies in the sections is presented. Third, the detrital zircon data are presented as combination histogram and probability density plots.

3.1 Mt. Wilson Measured Sections

The four measured sections from north to south (Figure 3) are: Wilcox Pass, Morberley Mountain, Kicking Horse Canyon, and Pedley Pass. During the process of measuring sections in the field, five distinct facies (Planar-bedded, "Leopard Rock, Massive-bioturbated, Large-scale trough cross-bedded, and Shale) were described (Table 1; Figures 4 and 5). A detailed description of the Mt. Wilson quartz arenite at each individual section follows.

3.1.1 Wilcox Pass Measured Section

The Wilcox Pass section (Figure 3) is approximately 60 m thick, and both the lower and upper contacts are covered. This section contained all five of the described facies with the cross-bedded quartz arenite facies being most abundant. The only shale in this section was near the middle. The stacking pattern of the facies is outlined in the discussion section. No samples were taken from this section as approval for sampling in a national park was not obtained prior to field work.

3.1.2 Morberley Mountain Measured Section

The Morberley Mountain section is approximately 247 m thick with the lower contact between the Mt. Wilson and the Glenogle Shale being exposed and the upper

contact being covered. This section was the thickest and most complex section measured for this study. All five facies were present with the massively bedded facies and the "Leopard Rock" facies being the most common (Figures 3 and 4). Shale occurred rarely in beds 1-3 m thick near the base of the section. Detrital zircon samples were taken at the base, middle, and top of the section.

3.1.3 Kicking Horse Canyon Measured Section

The Kicking Horse Canyon section (Figure 3) is approximately 117 m thick with the lower and upper contacts both covered. The large-scale cross-bedded facies was most abundant in this section, and both the "Leopard Rock" and shale facies were absent. The planar-bedded facies was the second most abundant facies, and this was the only section to have such a thick (20 m) occurrence of this facies. Detrital zircon samples were taken at the top and bottom of this section.

3.1.4 Pedley Pass Measured Section

The Pedley Pass section (Figure 3) was the thinnest section measuring approximately 18 m thick. Both its lower and upper contacts are exposed. The lower contact is a sharp surface between the Mt. Wilson and the Glenogle Shale. The upper contact between the Mt. Wilson and the Beaverfoot Formation also is a sharp surface. The massively-bedded facies (Figure 5) was the most abundant facies for this section, and the "Leopard Rock" facies was absent. A single detrital zircon sample was taken from the top of this section. All of these facies described here are presented in a block diagram as well (Figure 6)

3.2 Detrital Zircon Geochronology of Mt. Wilson Sections

A composite plot (Figure 7) of all six samples analyzed for the Mt. Wilson Formation was constructed using the same scale and format. An overview of this dataset indicates that all six samples have the following similarities:

a) The majority of Paleoproterozoic grains formed between 1.8 – 2.0 Ga,
b) The next large Paleoproterozoic population occurs between 2.0 – 2.2 Ga range; their proportion of the total population increases in the upper portion of the sections,
c) There is a persistent population of Paleoproterozoic-Archean (2.2 – 3.0 Ga) grains,
d) There are few grains of >3.5 Ga,
e) A smaller, younger, population of zircons occurs between 900 – 1200 Ma,
f) There is a very small (<5 grains) population of 1400-1600 Ma zircons distributed across half of samples.

4. DISCUSSION

4.1 Depositional Environments

Depositional environments (Figure 6) of the Mt. Wilson Quartzite are categorized by water depth and location relative to the shoreline, ranging from deep-water to shallow-water and far (distal) to near (proximal) location. The shale facies is interpreted to have formed in the deepest water and most distal environment (Schutter, 1998). The depositional environment of the large-scale trough cross-bedded facies is (Figure 6) lower shoreface, being more proximal than the shale and at slightly shallower water depth, where fair weather wave base was able to constantly move finer grained sediments basinward (Clifton, 2006). The massively bedded facies (Figure 6) is interpreted to have formed in the middle shoreface, a shallow water environment more proximal compared to the cross-bedded facies (MacEachern and Bann, 2008). A shallower water depth for this facies is inferred due to its abundant bioturbation. The "Leopard rock" facies (Figure 6) is subdivided as a facies because of its greater abundance of bioturbation, the increased size of its burrows, and the vertical nature of the burrowing indicating a Skolithos ichnofacies. The greater abundance and increased size of burrowing is interpreted to indicate a relative increase in biologic activity; however, this change may also record an increase in diagenesis or a change in size of organisms. Regardless, this unit is interpreted to have been deposited in the upper-middle shoreface a more shallow and proximal environment than the massive facies. Finally, the planar bedded facies (Figure 6) is interpreted to record a beach depositional environment, the most proximal, highest energy and shallowest water environment

(Plint, 2010). It is possible that these shallowest deposits could be eolian or non-marine because the progression of facies described is similar to a prograding wave-dominated shoreface (Plint, 2010), which is typically associated with a windblown environment. However, features associated with eolian deposits (i.e., reverse graded bedding, pinstripe wind ripples, large-scale trough cross-bedding; Kocurek, 1981) do not occur in this facies.

The Middle Ordovician St. Peter Sandstone also consists mainly of well-sorted, well-rounded quartz sand grains and those mature quartz arenites are interpreted to be first-cycle deposits, formed directly from weathering of basement rocks, not formed from recycled sedimentary rocks (Mai and Dott, 1985; Nadon et al., 2000). Similar first cycle quartz arenites are forming in the northern Amazon basin because of intense equatorial weathering (Johnsson et al., 1988). The Middle-Late Ordovician quartz arenites of western Laurentia were deposited near the paleoequator (Miall and Blakey 2003; Scotese, 2003), and their deposition along a passive margin dominated by carbonate rocks was enigmatic (Gehrels et al., 1995). The lack of detrital zircons sourced from recycled sedimentary rocks (see discussion below) and its depositional setting near the Late Ordovician equator suggests the Middle-Late Ordovician quartz arenites are first-cycle deposits.

4.2 Sequence Stratigraphy

Sequence stratigraphic interpretations indicate that important surfaces are typically identified by the vertical juxtaposition of two facies that are not normally deposited in succession (Catuneanu, 2006). Unconformities bound the Mt. Wilson

Quartzite indicating it recorded one full depositional sequence. Identifying unconformities within the Mt. Wilson Quartzite is difficult because these surfaces are more subtle than those used to develop the concepts of sequence stratigraphy (Mitchum and Van Wagoner, 1991). Using facies changes and stacking patterns, several surfaces were interpreted within the Mt. Wilson measured sections, and, these surfaces, along with facies stacking patterns were used to delineate its sequence stratigraphic framework (Figure 3). This includes a 2nd-order sequence (~8 Ma duration), two 3rd-order sequences (each approximately 4 Ma duration), and multiple parasequences (each a few hundreds of thousands of years duration). In each of the sections, surfaces marked by an abrupt change from relatively shallow facies to deeper facies were interpreted to be a sequence boundary (Figure 3) because it records a rapid change in depositional environment across a sharp surface (Mitchum and Van Wagoner, 1991). Sequence boundary 1 (SB1) occurs between the Mt. Wilson and either the underlying Owen Creek Formation or Glenogle Shale. Sequence boundary 2 (SB2) occurs between the Mt. Wilson Quartzite at its upper contact with the overlying Beaverfoot Formation. These two unconformities (Aitken et al., 1972) define a 2nd-order depositional sequence as the entire Mt. Wilson Quartzite recorded approximately 8 million years deposition (Pyle and Barnes, 2003). The Transgressive Systems Tract (TST) is interpreted to be everything below the highest occurrence of shale, usually within the first 25 m of the Mt. Wilson, and the remainder of the Mt. Wilson is interpreted to be the Highstand Systems Tract (HST). The most significant facies change in the Mt. Wilson Quartzite is interpreted to be a sequence boundary (SB1a) and suggests the Mt. Wilson quartz arenite records two 3rd-order

sequences. The lower 3rd-order sequence begins at the base of the Mt. Wilson Quartzite where it was deposited unconformably upon the Owen Creek Formation or Glenogle Shale. Above this, the TST was deposited, mostly consisting of shale overlain by rocks that record a deepening in water depth, until the maximum flooding surface (MFS1a). This surface is the MFS1a and is the contact above the deepest water facies in the lower part of the Mt. Wilson. Above the MFS1a, the HST was deposited, consisting of a succession of shallowing upward facies. This 3rd-order sequence continues until sequence boundary SB1a which, in the Morberley Mountain section, is located between the first appearance of "Leopard Rock" and the overlying large-scale trough cross-bedded facies. The upper 3rd-order first consists of the TST, which, includes a deepening upward sequence of deposits capped with a maximum flooding surface (MFS2a). Above the MSF2a is a shallowing upward succession of facies and this 3rd-order sequence ends at the SB2. Several parasequences (Figure 3), recording shallowing- or deepening upward facies associations, occur throughout the Mt. Wilson quartz arenite, but none of them is correlated regionally. Generally the TSTs of the 3rd-order sequences consist of 1-3 deepening upward parasequences, and, in the HSTs there are 1-3 shallowing upward parasequences. These correlations span multiple thrust sheets (Price, 1994), and without more detailed biostratigraphic constraints and more, closer spaced measured sections it is difficult to correlate, even 3rd-order sequences regionally.

4.3 Detrital Zircon Provenance

Populations of detrital zircon (dz) grains in sedimentary rock units are commonly used to identify possible provenance areas (Gehrels et al., 1995; Gehrels, 2000). The Mt.

Wilson Quartzite was sampled at three geographic locations and different stratigraphic levels to determine if temporal and spatial changes in provenance of this unit could be discerned.

4.3.1 Possible provenance areas

A composite basement map (Hammer, 2011; Figure 8) was used to aid in identifying possible provenance areas for the Mt. Wilson Quartzite. Zircons ca. 900 – 1100 Ma were produced during the Grenville Orogeny; rocks associated with this orogeny were exposed along the east coast of Laurentia and were re-distributed by a continental-scale fluvial system to the northern portion of Laurentia (Rainbird et al., 1992). The 900-1200 Ma grains in the Mt. Wilson quartz arenite were most likely reworked from these older sediments. 1400 – 1500 Ma zircons occur in several pre-Grenville plutons distributed from modern-day New Mexico to the west coast of the United States near the Ordovician Laurentian margin (Dickinson, 2008). A possible method for getting these grains to this unit would be erosion of those plutons located to the east of the depositional area by local rivers. 1600 – 1700 Ma zircons occur in the Yavapai-Mazatzal belts (Dewitt, 1989) located along the southern Laurentian margin. These are also the dominant grains in the lower Muskwa assemblage and the Belt-Purcell Supergroup (Ross et al., 1992; Ross et al., 2001; Ross and Villeneuve, 2003). It is more likely that the limited number of these zircon grains in the Mt. Wilson Quartzite were re-worked from these proximal sedimentary sources, rather than from southern areas. Rocks of this age also occur in the Taltson terrane (Hammer, 2011) located along the northern Ordovician Laurentian margin. This represents a more local provenance due

to its proximity to the purported depositional source area for the Mt. Wilson quartz arenite. The likely method of transport would be proximal fluvial systems eroding exposed Taltson rocks. 1800 – 2000 Ma zircons occur in the terrane Trans-Hudson Orogeny terrane (Ansdell et. al, 1995; Hollings and Ansdell, 2002; St-Onge et. al, 2007). These zircons could also fall in the range of the Taltson terrane, which is more proximal to the depositional location. 2000 – 2400 Ma zircons are associated with the Buffalo Head Terrane (northern Alberta; Ross and Eaton, 2002), Paleoproterozoic Crust (southeast Wyoming; Mueller and Frost, 2006), and the Wopmay Terrane (western Canadian shield; Hammer, 2011). 2400 – 2500 Ma zircons formed in basement rocks associated with the Nistowiak thrust belt that is exposed in knappes of the Trans-Hudson Orogeny (Chiarenzelli et. al, 1998). 2500 Ma and older rocks in many portions of the craton were exposed during the Ordovician (Witzke, 1990). These include the Slave craton (Hammer, 2011) of the northern Canadian shield, Superior Craton (Condie et al., 2008), and Wyoming Craton (Hammer, 2011) of the southern Canadian shield.

Based on the age populations of these samples, the likely provenance areas (Figure 8) are those associated with the largest peaks on the probability density plots (Figure 7; 1.8 – 2.0 Ga and 2.0 – 2.1 Ga). Source areas that had these age rocks exposed during Middle-Late Ordovician include: northern Alberta (northeast of Mt. Wilson Quartzite), southern Alberta (east of Mt. Wilson Quartzite, and the Idaho and Montana area (southeast of Mt. Wilson Quartzite). The Transcontinental Arch was located in southern Alberta, Idaho, Montana, and, was topographically high relative to surrounding areas. The simplest explanation for similarities between detrital zircon populations of the

Mt. Wilson Quartzite and basement terranes exposed on the Transcontinental Arch would be a system of rivers and tributaries that distributed sediment near the depositional area of the unit. The existence of both a large proportion of zircons of same age as rocks associated with the Trans-Hudson Orogen and a small proportion of zircons of same age as the rocks exposed in knappes in the same area further supports this east/southeast provenance area.

4.3.2 Changes in Provenance

Changes in provenance are inferred from changes in relative proportionality of zircon grains from lower parts of sections to the upper parts of sections. However, based on the statistical analysis of detrital zircon populations, no significance is given to changes involving the inclusion or exclusion of single zircon grains (Sircombe, 2000).

The sub-population of 2000-2200 Ma zircons (Figure 7) increases in number from the lower Morberley Mountain sample to the upper Morberley Mountain sample. This increase is interpreted to record a greater percentage of sediment was derived from terranes of this age at the expense of surrounding terranes. Because these terranes are located farther from the study area than other terranes, it indicates that the terranes available for erosion where further inland, suggesting these rocks record a sea level rise to access these terranes. A rise in sea level during the time of deposition of the upper portion of the Mt. Wilson coincides with increased continental flooding of Laurentia during the Cincinnatian (Algeo and Seslavinsky, 1995; Xhen and Barnes, 2008;). This supports a temporal change in provenance of the Mt. Wilson quartz arenite, and, indicates the effect of long-term relative sea-level change on this unit's provenance.

Spatial changes in provenance between sections of the Mt. Wilson Quartzite are not clear and further analysis of different samples from the Mt. Wilson would be required to document them. Because any spatial changes in provenance that exist within this unit are likely subtle, statistical analysis of data is needed. One method of investigating spatial changes is to compare data from the same rock unit but from different areas using statistical overlap and similarity (Gehrels, 2000). Both overlap and similarity are on a scale from 0 (no overlap/similarity) to 1 (perfect overlap/similarity). Overlap is the presence of an age in both samples being compared and similarity uses the square root of the product of the pair of probabilities (Fedo et al., 2003). When our data from individual sections is compared to data from a Mt. Wilson Quartzite sample from a different locality (Gehrels et al., 1995) there is a range in overlap value from 0.497 – 0.842 and similarity ranges from 0.798 – 0.917 (Table 2). Based on the ranges of values, there appears to be a correlation between population size and overlap value while there seems to be no correlation between population size and similarity value. In both overlap and similarity, the Pedley Pass sample has the lowest value, and, because it does not have enough grains to be considered statistically adequate (between 60-117; Vermeesch, 2004) it is only included in this discussion of the statistical analysis in passing. Neglecting the Pedley Pass data, the overlap and similarity values between sections and with the reference section provided by George Gehrels the values are high. Comparison of the three samples reveals that the two sections closest to each other (MM and KHC) have higher values than when compared to PP, which is a greater distance away. These results suggest that the spatial change between sections of the Mt. Wilson Quartzite is

negligible and likely an artifact from the small size of the Pedley Pass sample. Also, any sections sampled in the future, if population size is adequate, would likely have a similar detrital zircon population.

4.3.3 Summary

The Mt. Wilson quartz arenites and other Mid-Late Ordovician quartz arenites are important to study for several reasons. First, the detrital zircon data in this study and other studies indicate that the detrital zircon signature of these units are unique when compared to overlying and underlying units of the western Laurentian margin (Gehrels et al., 1995; Gehrels, 2000; Pope et al., 2011). Also, the deposition of siliciclastic units in the middle of a carbonate dominated passive margin is enigmatic, making any information about such units important.

As a first-cycle deposit, the Mt. Wilson Quartzite has a detrital zircon population that most likely represents primarily igneous and metamorphic sources along the Transcontinental Arch, not reworked sedimentary sources along the periphery of Laurentia. Possible sedimentary sources near the study area (e.g. the lower Muskwa assemblage and the Belt-Purcell Supergroup) have large younger zircon populations (e.g. 1.6-1.8 Ga and 1.07-1.24 Ga; Ross et al., 1992; Ross et al., 2001). The sparse number of these age grains in the Mt. Wilson Quartzite indicates that recycling of these sedimentary rocks was not an abundant sediment source.

The numerous possible provenance areas in western Canada that exclude the Peace River Arch, combined with the Mt. Wilson Quartzite being a first-cycle deposit, make a strong case against the Peace River Arch being a point source for all other Middle-Late Ordovician quartz arenites of western Laurentia

5. CONCLUSIONS

Through detailed description of measured sections, depositional facies were defined for the Mt. Wilson Quartzite. Depositional environments of this first-cycle deposit, are listed from deepest to shallowest water environment: shale facies, large-scale trough cross-bedded facies, massive-bioturbated facies, "Leopard Rock" facies, and planar-bedded facies. The stacking patterns of these facies were used to develop the sequence stratigraphic framework that indicates the Mt. Wilson Quartzite is an unconformity bounded 2nd-order depositional sequence, containing two 3rd-order sequences, and many parasequences.

Detrital zircon data from the Mt. Wilson Quartzite combined with detailed measured sections and facies description were used to identify possible provenance areas in northern Canada and changes in provenance over time. The main peaks in the data, 1800-2000 Ma, 2000-2200 Ma, and 2300-2400 Ma are interpreted to derive from terranes east of the study area: Trans-Hudson Orogeny (1800-2000 Ma), Taltson (1800-2000 Ma), Buffalo Head Terrane (2000-2400 Ma), Paleoproterozoic crust (2000-2400 Ma), and the Wopmay Terrane (2000-2400 Ma). It is likely that these basement areas were sourced by local rivers and tributaries draining the Transcontinental Arch and distributed sediment in the deposition area of the Mt. Wilson Quartzite. Longshore transport likely moved sediment laterally along the passive margin providing similar detrital zircon signatures amongst Middle-Late Ordovician quartz arenites. However, our data do not support the Peace River Arch as a point source for these units. Changes in detrital zircon signatures from lower to upper samples within measured sections suggest

a long-term flooding produced a slight change in provenance as terranes were flooded and rivers reached accessed basement units further inland. Statistical comparison of the different signatures of measured sections suggests that any spatial change in provenance was negligible and unlikely to be detected by studies of detrital zircons.

REFERENCES

Aitken, J.D., Fritz, W.H., and Norford, B.S. 1972. Cambrian and Ordovician biostratigraphy of the southern Canadian Rocky Mountains of Alberta. Ottowa, 24th International Geological Congress, Guidebook for Excursion, A19: 57 p.

Algeo, T. and Seslavinsky, K. 1995. The Paleozoic World: Continental flooding, hyposemetry, and sea level. American Journal of Science, **295**: 787-822.

Ansdell, K.M., Lucas, S.B., Connors, K., and Stern, R.A. 1995. Kisseynew metasedimentary gneiss belt, Trans-Hudson orogeny (Canada): Back-arc origin and collisional inversion. Geology, **23**(11): 1039-1043.

Catuneanu, O. 2006, Principles of sequence stratigraphy, Boston, Elsevier.

DeWitt, E. 1989. Geochemistry and tectonic polarity of Early Proterozoic (1700-1750 Ma) plutonic rocks, north-central Arizona. *In* Geologic evolution of Arizona. *Edited by* J. P. Jenny and S. J. Reynolds, Tuscon, Arizona Geological Digest, **17:** 149-163.

Cecile, M.P. and Norford, B.S. 1991. Ordovician and Silurian assemblages. Chapter 7 *In* Geology of the Cordilleran Orogen in Canada. *Edited by H.* Gabrielse and C.J. Yorath, Geological Survey of Canada, Geology of Canada, **4:** 184-196.

Chang, Z., Vervoort, J.D., Knaack, C., and McClelland, W.C. 2006, U-Pb dating of zircon by LA-ICPMS. Geochemistry, Geophysics, Geosystems, **7**(5): 1-14. Q05009, doi:10.1029/2005GC001100.

Chiarenzelli, J., Aspler, L., Villeneuve, M., Lewry, J. 1998. Early Proterozoic evolution of the Saskatchewan Craton and its allocthonous cover, Trans-Hudson Orogen. Geology, **106**: 247-267.

Clifton, H.E. 2006. A reexamination of facies models for clastic shorelines. *In* Facies models revisited. *Edited by R.G.* Posamentier and R.G. Walker, SEPM Special Publication **84.** pp. 237292.

Davis, D.W., Hirdes, W., Schaltegger, U., and Nunoo, E.A. 1994, U-Pb age constraints on deposition and provenance of Birmian and gold-bearing Tarkwaian sediments in Ghana, West Africa. Precambrian Research, **67**: 89-107.

Dickinson, W.R. 2008. Impact of differential zircon fertility of granitoid basement rocks in North America on age populations of detrital zircons and implications for granite petrogenesis. Earth and Planetary Science Letters, **275**(1-2): 80-92. doi: 10.1016/ j.epsl.2008.08.003.

Dodson, M.H., Compston, W., Williams, I.S., and Wilson, J.F. 1988. A search for ancient detrital zircons in Zimbabwean sediments. Journal of the Geological Society of London, **145:** 977-983.

Fedo, C. M., Sircombe, K.N., and Rainbird, R.H., 2003, Detrital zircon analysis of the sedimentary record. *In* Zircon. *Edited by J.M.* Hanchar and P.W.O. Hoskin, Reviews in Mineralogy and Geochemistry, **53:** 277-303.

Gehrels, G.E., 2000 Introduction to detrital zircon studies of Paleozoic and Triassic strata in western Nevada and northern California. *In* Paleozoic and Triassic Boulder, CO. *Edited by* M.J. Soreghan and G.E. Gehrels, Geological Society of America Special Paper 347, pp. 1-17.

Gehrels, G.E., Dickinson, W.R., Ross, G.M., Stewart, J.H., and Howell, D.G., 1995, Detrital zircon reference for Cambrian to Triassic miogeoclinal strata of western North America: Geology, **23:** 831-834.

Hammer, P.T.C., Clowes, R.M., Cook, F.A., Vasudevan, K., and van der Velden, A.J. 2011. The big picture: lithospheric cross section of the North American continent. GSA Today, **21**(6): 4-10.

Hoffman, P.F. 1992. Supercontinents. *In* Encyclopedia of Earth System Science. *Edited by* W.A. Nierenberg, London, Academic Press, **4**: 323-327.

Hollings, P., and Ansdell, K. 2002. Paleoproterozoic arc magmatism imposed on an older backarc basin: Implications for the tectonic evolution of the Trans-Hudson orogeny, Canada. GSA Bulletin, **114**(2): 153-168.

Irving, E., and McGlynn, J.C. 1976. Proterozoic magnetostratigraphy and the tectonic evolution of Laurentia. Philosophical Transactions of the Royal Society of London. A **280**(1298): 433-468.

Johnsson, M.J., Stallard, R.F., and Meade, R.H. 1988. First-cycle quartz arenites in the Orinoco River Basin, Venezuela and Colombia. Journal of Geology, **96**(3): 263- 267.

Ketner, K.B. 1968. Origin of Ordovician Quartzite in the Cordilleran Miogeosyncline. United States Geological Survey Professional Paper 600-B, pp. B169-B177.

Kocurek, G. 1981. Significance of interdune deposits and bounding surfaces in Aeolian dune sands. Sedimentology, **28**(6): 753-780. doi: 10.1111/j.1365-3091.1981.tb01941.x

Ludwig, K.R. 2003. User's Manual for Isoplot 3.00: a geochronological toolkit for Microsoft Excel. Berkeley Geochronology Center, Berkeley, Calif., Special Publication 4. 71 p.

MacEachern, J.A. and Bann, K.L. 2008. The role of ichnology in refining shallow marine facies models. *In* Recent Advances in Models of Siliciclastic Shallow-Marine Stratigraphy. *Edited by G.J.* Hampson, R.J. Steel, P.M. Burgess, and R.W. Dalrymple, SEPM Special Publication **90**. Pp. 73-116.

Mai, H., and Dott Jr., R.H. 1985. A subsurface study of the St. Peter Sandstone in Southern and Eastern Wisconsin. Wisconsin Geological and Natural History Survey, Information Circular number 47. p. 35.

Miall, A.D., and Blakey, R.C. 2008. Chapter 1 The Phanerozoic tectonic and sedimentary evolution of North America. *In* Sedimentary Basins of the World. *Edited by* A.D. Miall, Elsevier, **5:** 1-29. doi: 10.1016/S1874-5997(08)00001-4.

Mitchum Jr., R.M., and Van Wagoner, J.C. 1991. High-frequency sequences and their stacking patterns: sequence-stratigraphic evidence of high-frequency eustatic cycles. Sedimentary Geology, **70**(2-4): 131-14.

Mueller, P.A., and Frost, C.D. 2006. The Wyoming Province: a distinctive Archean craton in Laurentian North America. Canadian Journal of Earth Sciences, **43**(10): 1391-1397. doi: 10.1139/e06-075.

Nadon, G.C., Simo, J.A.T., Dott, R.H., and Byers, C. W. 2000. High-resolution sequence stratigraphic analysis of the St. Peter Sandstone and Glenwood Formation (Middle Ordovician), Michigan Basin, U.S.A. AAPG Bulletin, **84**(7): 975-996.

Norford, B. S. 1969. Ordovician and Silurian stratigraphy of the southern Rocky Mountains. Canada Geological Survey Bulletin 176-180, **176**: 90.

Plint, A.G. 2010. Wave- and storm-dominated shoreline and shallow-marine systems. *In* Facies Models 4. *Edited by* James, N.P., and Dalrymple, R.W., Geological Association of Canada, GEOtext, **6**. pp. 167-199.

Pope, M.C., Baar, E.E., Hutto, A., Workman, B., Wulf, T., Pickell, M.J. 2011. 2nd- and 3rd-order sequence stratigraphy, depositional environments, and provenance of middle-late Ordovician supermature quartz arenites, North America. Geological Society of America Abstracts with Programs, **43**(5): p. 205.

Price, R.A. 1994. Cordilleran tectonics and the evolution of the Western Canada Sedimentary Basin. *In* Geological Atlas of the Western Canada Sedimentary Basin. *Compiled by G.D.* Mossop and I. Shetsen, Calgary, Canadian Society of Petroleum Geologists and Alberta Research Council, chpt. 2.

Pyle, L.J., and Barnes, C.R. 2003. Lower Paleozoic stratigraphic and biostratigraphic correlations in the Canadian Cordillera: implications for the tectonic evolution of the Laurentian margin. Canadian Journal of Earth Sciences, **40**: 1739-1753. doi: 10.1139/E03-049.

Rainbird, R.H., Hearnan, L.M., Young, G. 1992. Sampling Laurentia: Detrital zircon geochronology offers evidence for an extensive Neoproterozoic river system originating from the Grenville orogen. Geology, **20**: 351-354. doi: 10.1130/0091-7613(1992) 020<0351:SLDZGO>2.3.CO; 2.

Roback, R.C., and Walker, N.W. 1995. Provenance, detrital zircon U-Pb geochronometry, and tectonic significance of Permian to Lower Triassic sandstone in southeastern Quesnellia, British Columbia and Washington. Geological Society of America Bulletin, **107**: 665-675.

Ross, G.M., Parrish, R.R., and Winston, D. 1992. Provenance and U-Pb geochronology of the Mesoproterozoic Belt Supergroup (northwestern United States): implications for age of deposition and pre-Panthalassa plate reconstructions. Earth and Planetary Science Letters, **113**: 57-76.

Ross, G.M., Villeneuve, M.E., and Theriault, R.J. 2001. Isotopic provenance of the lower Muskwa assemblage (Mesoproterozoic, Rocky Mountains, British Columbia): new clues to correlation and source areas. Precambrian Research, **111**(1-4): 57- 77.

Ross, G.M., and Eaton, D.W. 2002 Proterozoic tectonic accretion and growth of western Laurentia: Results from Lithoprobe studies in northern Alberta. Canadian Journal of Earth Sciences, **39**(3): 313-329. doi: 10.1139/e01-081.

Schutter, S.R. 1998. Characteristics of shale deposition in relation to stratigraphic sequence systems tracts. *In* Shales and mudstones; I, Basin studies, sedimentology, and paleontology. *Edited by* J. Schieber, W. Zimmerle, and P.S. Sethi, Stuttgart, Schweizerbart, pp. 79-108.

Scotese CR. 2003. Paleomap Project. URL http://www.scotese.com/Default.htm URL

Scott, D.J., and Gauthier, G. 1996. Comparison of TIMS (U-Pb) and laser ablation microprobe ICP-MS (Pb) techniques for age determination of detrital zircons from Paleoproterozoic metasedimentary rocks from northeastern Laurentia, Canada, with tectonic implications. Chemical Geology, **131:** 127-142.

Sircombe, K.N. 2000. Quantitative comparison of geochronological data using multivariate analysis: a provenance study example from Australia. Geochemica et Cosmochimica Acta, **64:** 1593-1619.

St-Onge, M.R., Wodicka, N., and Ijewliw, O. 2007. Polymetamorphic evolution of the Trans-Hudson orogeny, Baffin Island, Canada: Integration of petrological, structural and geochronological data. Journal of Petrology, **48**(2): 271-302. doi:10.1093/ petrology/egl060.

Sweet, W.C. 2000. Conodonts and biostratigraphy of Upper Ordovician strata along a shelf to basin transect in Central Nevada. Journal of Paleontology, **74:** 1148- 1160.

Vermeesch, P. 2004. How many grains are needed for a provenance study? Earth and Planetary Science Letters, **224**: 441-451.

Webb, G.W. 1958. Middle Ordovician stratigraphy in eastern Nevada and western Utah. American Association of Petroleum Geologists Bulletin, **42**(10): 2335-2377.

Whitmeyer, S.J., and Karlstrom, K.E. 2007. Tectonic model for the Proterozoic growth of North America. Geosphere, **3**(4): 220-259. doi: 10.1130/GES00055.1.

Witzke, B. J. 1990. Paleoclimatic constraints for Paleozoic paleolatitudes of Laurentia and Euramerica. *In* Paleozoic paleogeography and biogeography. *Edited by* W.S. Mckerrow, and C.R. Scotese, London, Geological Society, Memoir 12: pp. 5773.

APPENDIX A

TABLES AND FIGURES

Table 1. Summary of Facies. Mt Wilson Quartzite Facies Descriptions and Interpretations.

Facies	Description	Interpretation
Planar-bedded quartz arenite	Light grey weathers to dark grey, very fine lower to very fine upper sized grains. Low-angle laminated sandstone. Bed thickness ~ 10 cm.	Beach/foreshore depositional environment, shallowest water facies (Plint, 2010).
"Leopard Rock"	Light grey weathers to light brownish grey, very fine upper sized grains, large-scale diagenetically enhanced burrows. Some elements of Skolithos ichnofacies.	Upper shoreface depositional environment (Plint, 2010; MacEachern and Bann, 2008).
Massively-bedded, bioturbated quartz arenite	Light grey weathers to dark grey, very fine upper sized grains. Some small-scale trough cross-bedding.	Middle shoreface depositional environment (MacEachern and Bann, 2008).
Large-scale cross-bedded quartz arenite	Light yellowish white weathers to brownish gray, very fine lower to very fine upper sized grains. Bed thickness from 10 cm – 40 cm.	Lower shoreface depositional environment (Clifton, 2006).
Shale	Brownish gray interbedded with sand. Bed thickness from 1 cm – 10 cm	Offshore depositional environment, deepest water facies (Schutter, 1998).

Table 2. Overlap and Similarity.

		OVERLAP		
Gehrels	**Gehrels**			
PP	0.497	**PP**		
KHC	0.811	0.399	**KHC**	
MM	0.842	0.468	0.790	**MM**
ALL	0.842	0.413	0.935	0.853

		SIMILARITY		
Gehrels	**Gehrels**			
PP	0.798	**PP**		
KHC	0.917	0.807	**KHC**	
MM	0.892	0.834	0.910	**MM**
ALL	0.915	0.842	0.942	0.944

Note: Gehrels. data from Gehrels et al., 1995; PP, Pedley Pass; KHC, Kicking Horse Canyon; MM, Morberley Mountain; ALL, All data from this study.

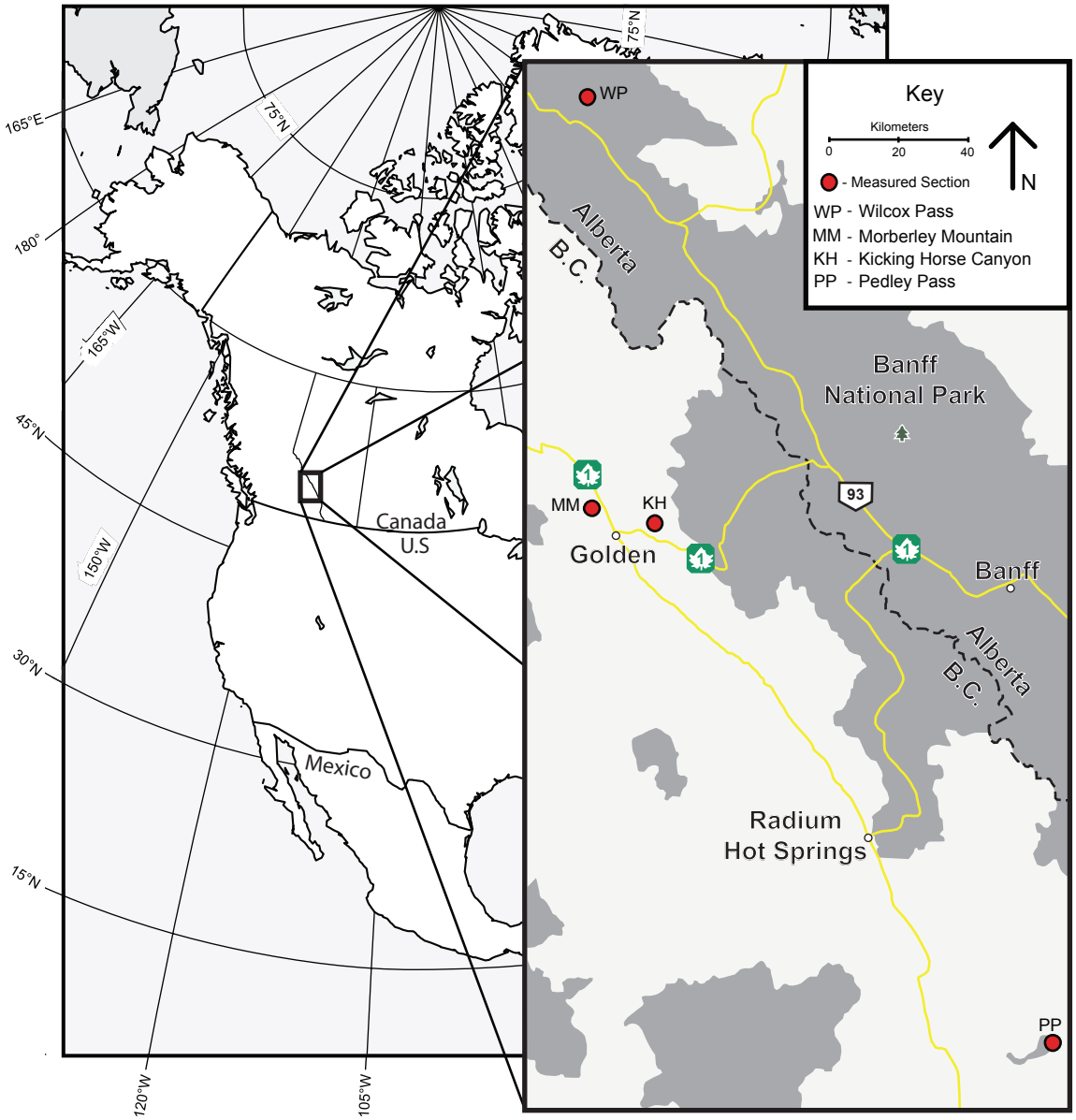

Fig. 1. Location of Study Area. Map showing locations of measured sections in study area, referenced to North America (modified from Google Maps, 2011).

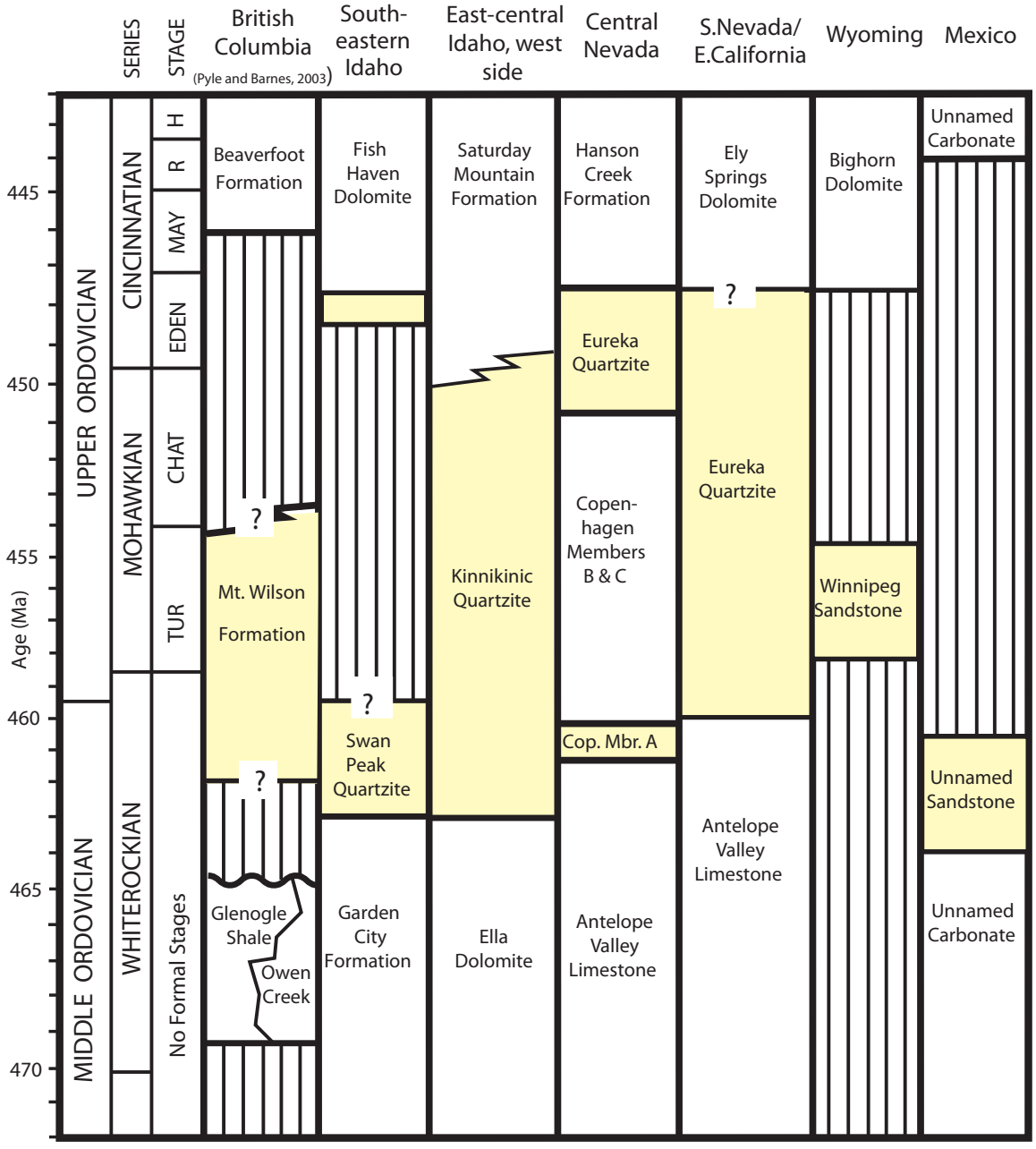

Fig. 2. Chronostratigraphic Cross Section. Compares mid-late Ordovician quartz arenites from North America. Based on current biostratigraphic correlations.

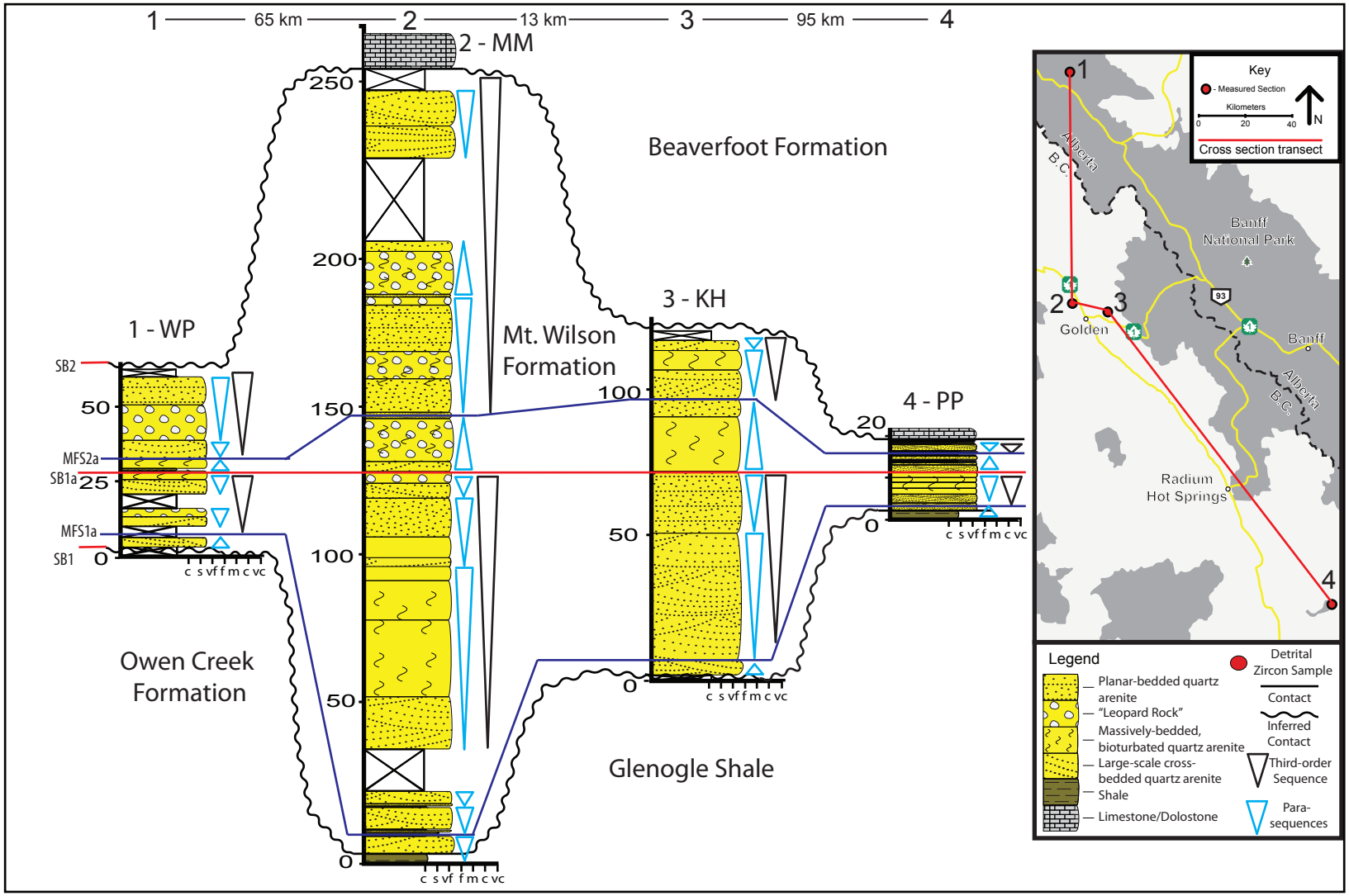

Fig. 3. Cross Section. Correlated through four Mt. Wilson Quartzite measured sections. Shows upper and lower contacts, formation names, facies, and sequence stratigraphic correlations.

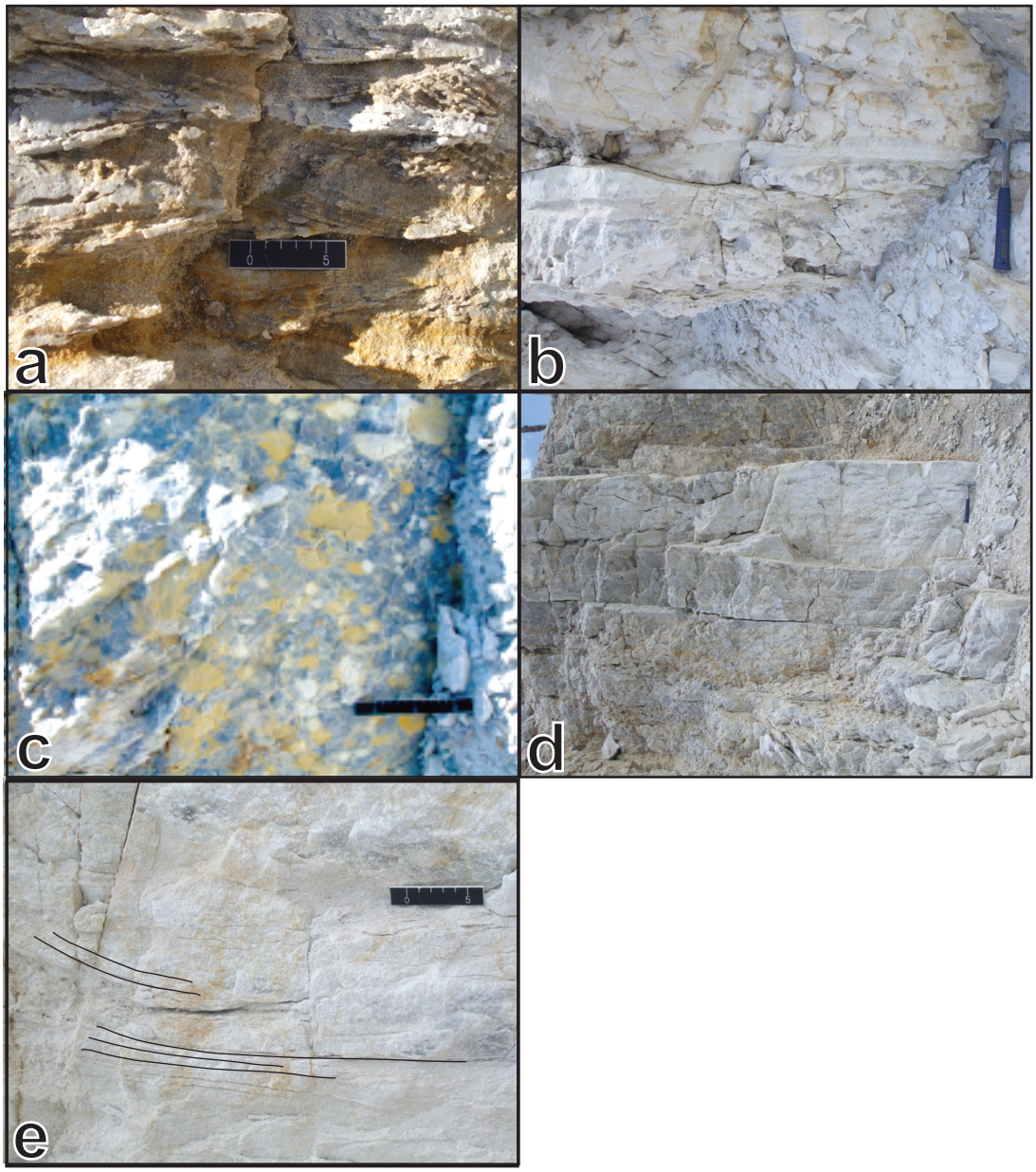

Fig. 4. Outcrop Pictures of Morberley Mountain. Section of Mt. Wilson quartz arenite. Scale bar is 5 cm in length. a.) Small-scale trough cross-bedding; b.) Massively bedded quartz arenite; c.) Large-scale diagenetically enhanced burrows; d.) Large scale planar bedding; e.) Small-scale trough cross-bedding.

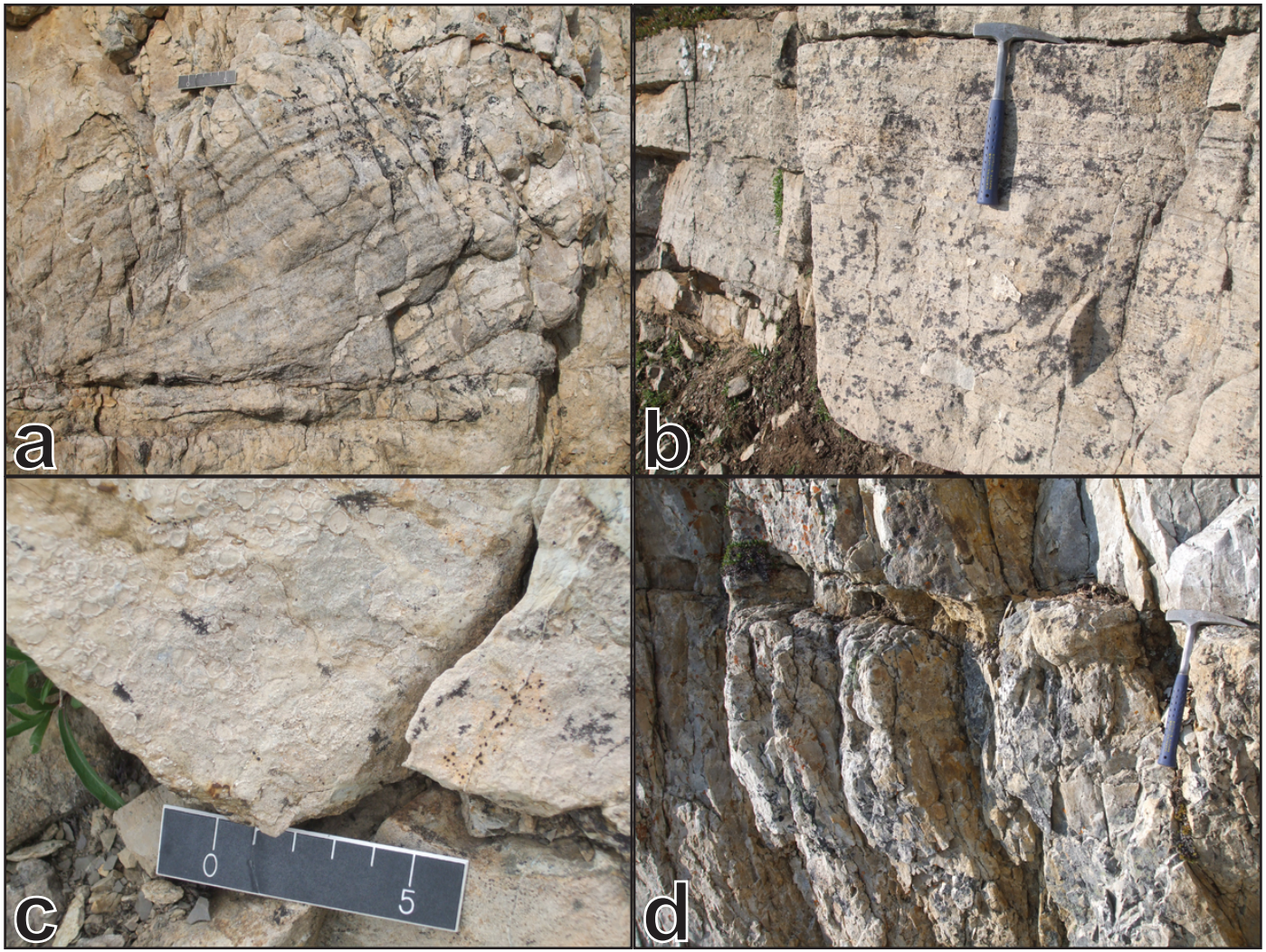

Fig. 5. Outcrop Pictures of Pedley Pass. Scale bar is 5 cm long and hammer is 28 cm long. a.) Large scale trough cross-bedding, b.) Large scale trough cross-bedding, c.) Low-angle planar cross-bedding, d.) Massive bedding.

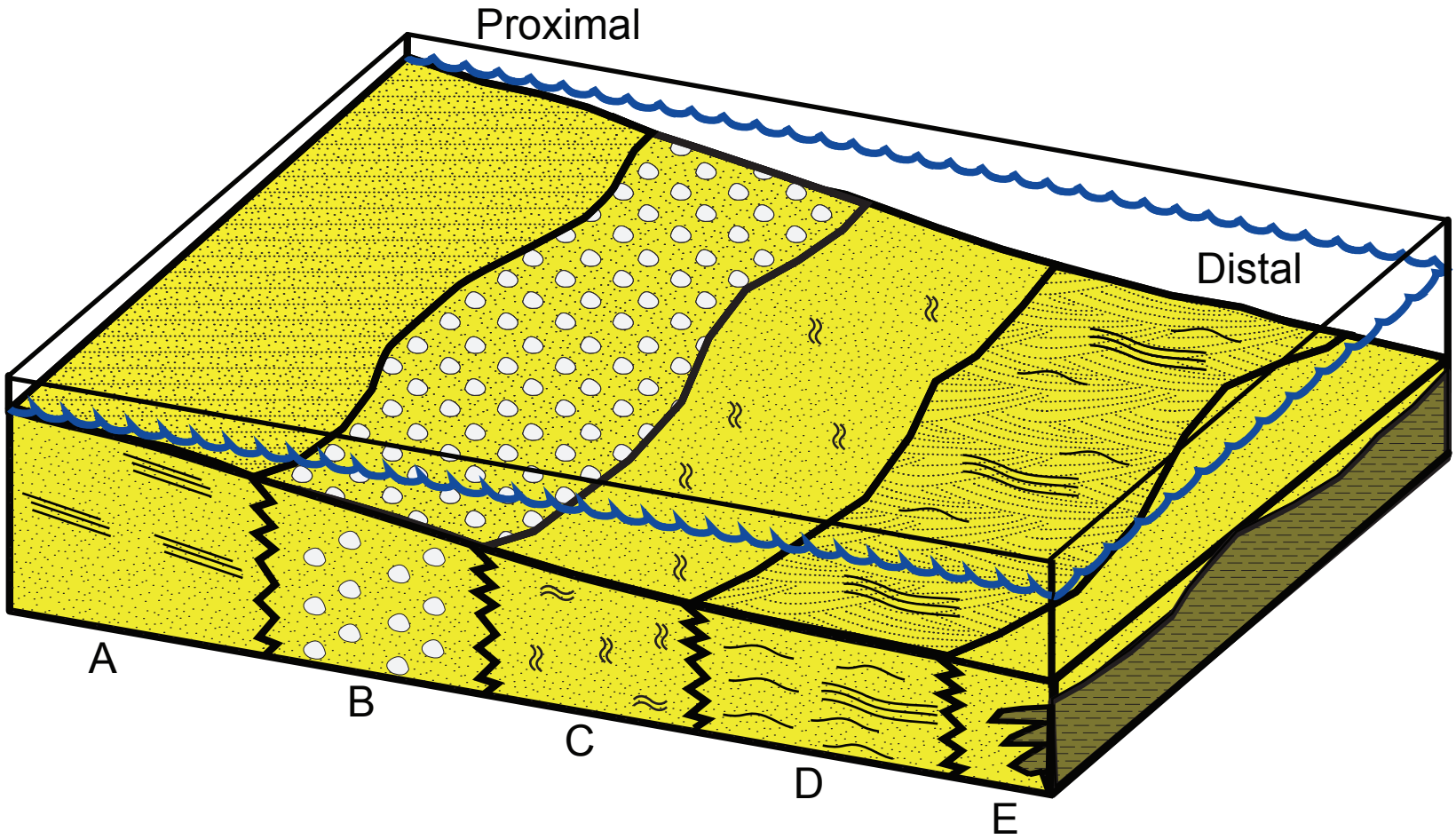

Fig. 6. Depositional Facies Block Diagram. Schematic illustrating the lateral relationships of the facies described in this thesis.

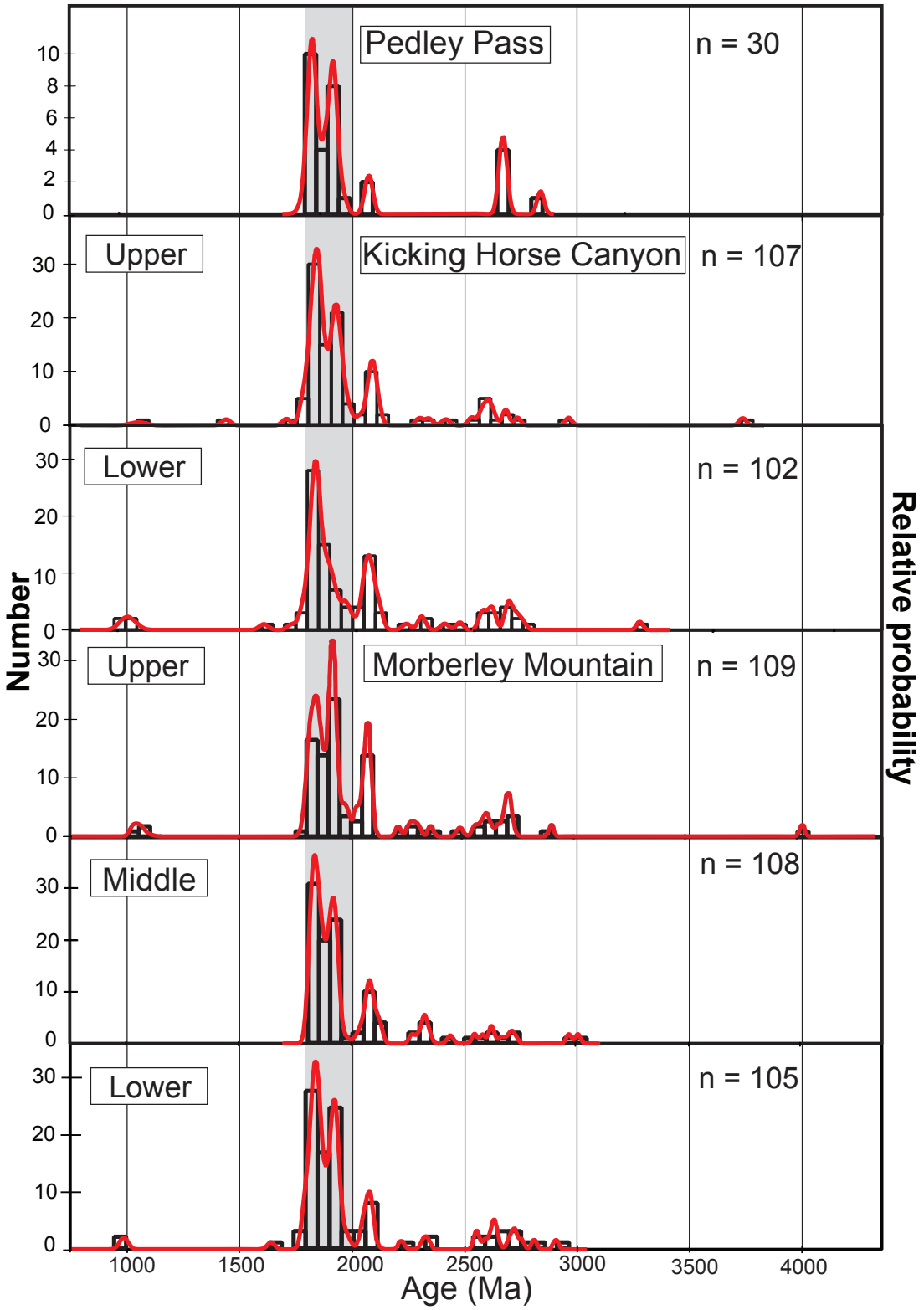

Fig. 7. Probability Density Plots of Samples. Zircon data from all Mt. Wilson Quartzite samples in this thesis. Displayed using both probability density and histogram plots.

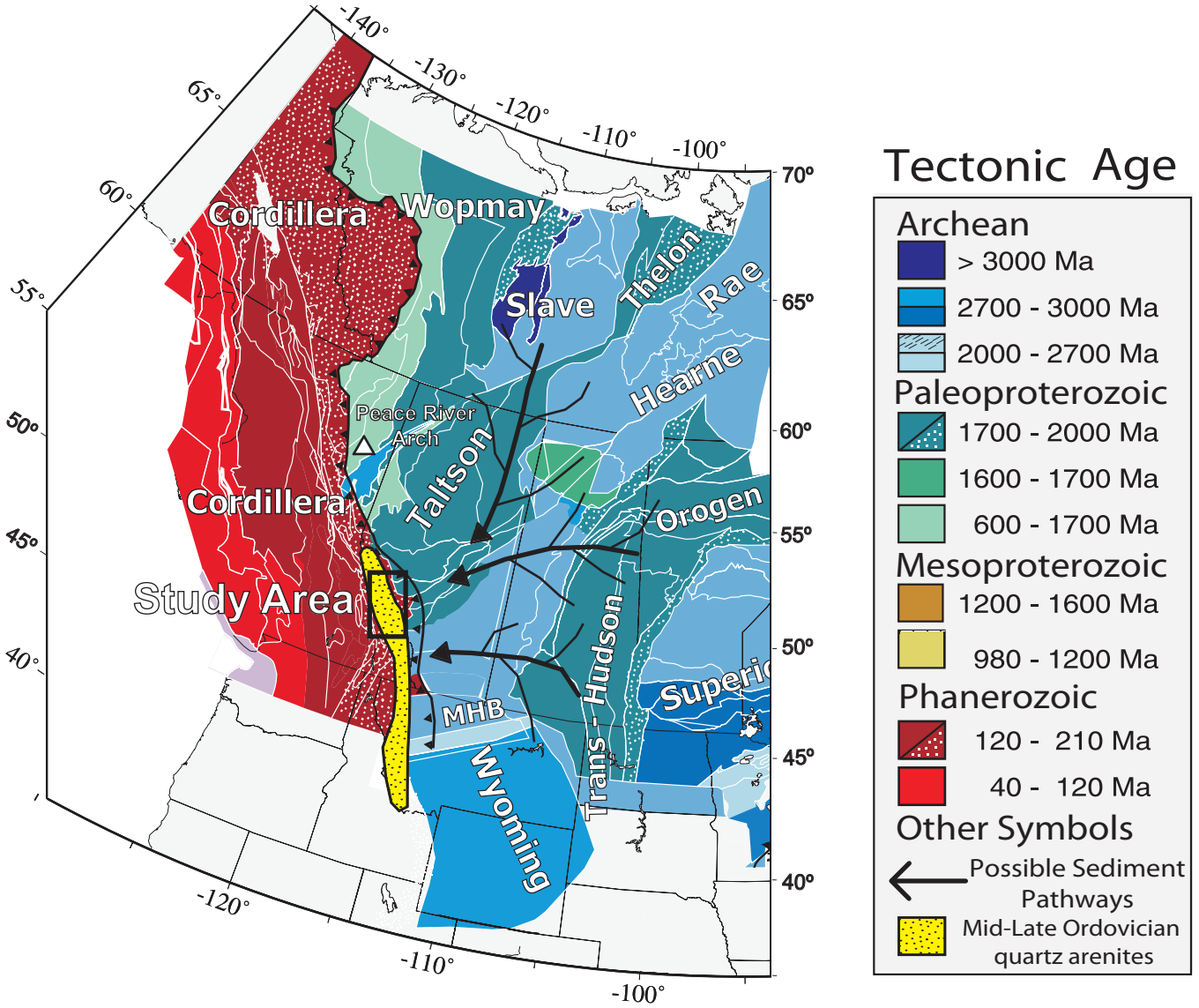

Fig. 8. Tectonic Terranes Map. Western Canada. Also illustrates possible sediment dispersal pathways.

APPENDIX B

DETAILED MEASURED SECTIONS

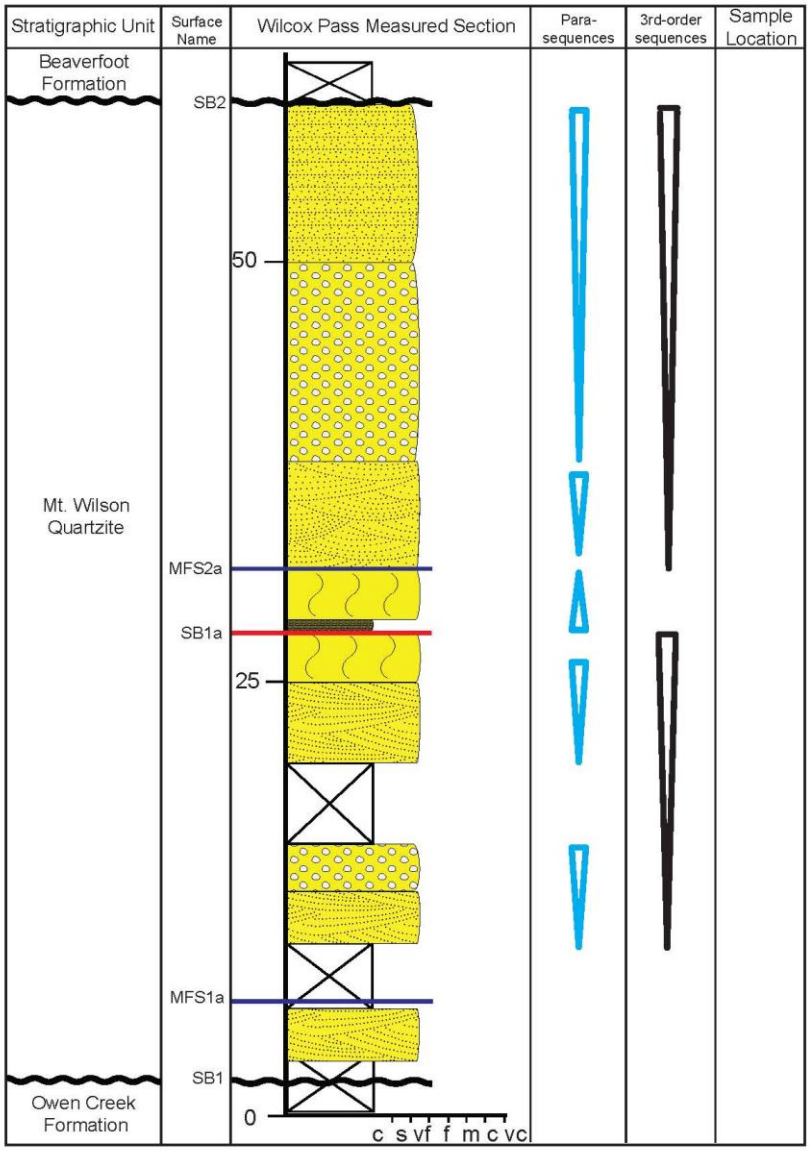

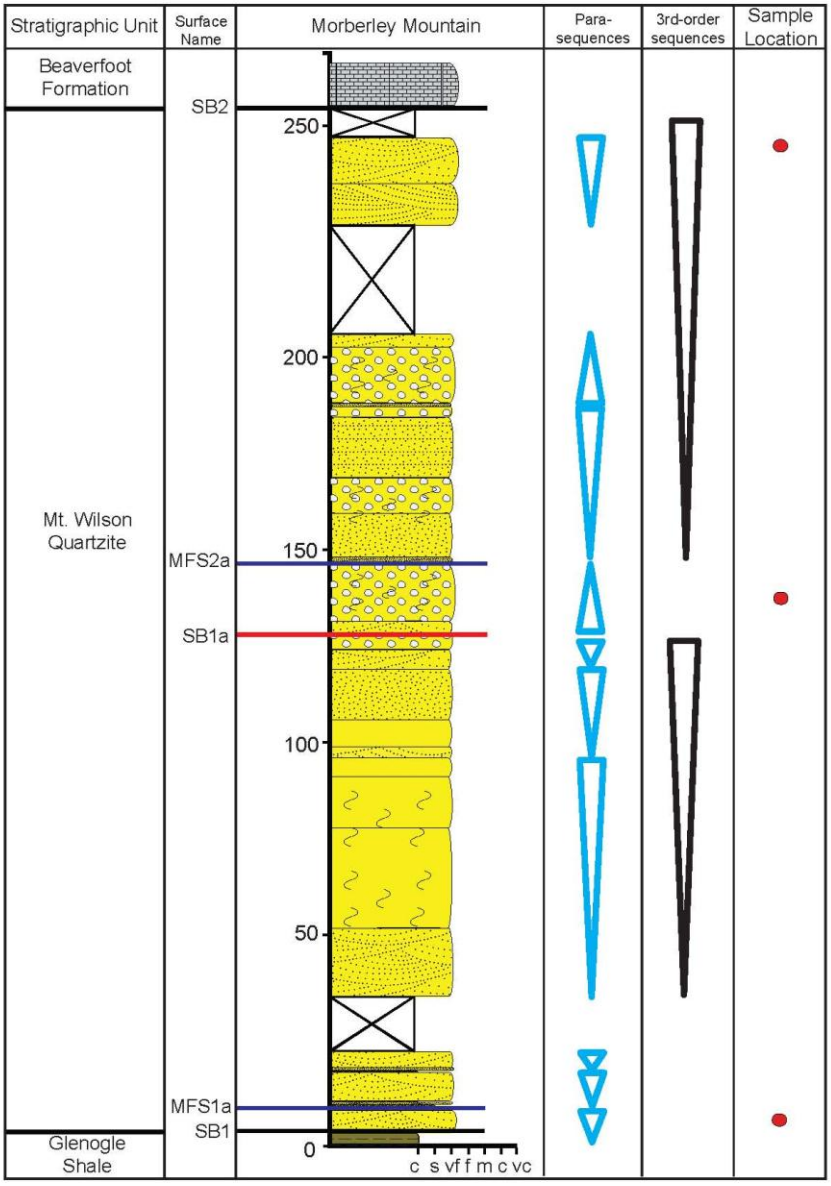
Stratigraphic Unit
Surface Name
Morberley Mountain
Para-sequences
3rd-order sequences
Sample Location
Beaverfoot Formation
SB2
250
200
Mt. Wilson Quartzite
150
MFS2a
SB1a
100
50
MFS1a
SB1
Glenogle Shale
0
c s vf f m c vc

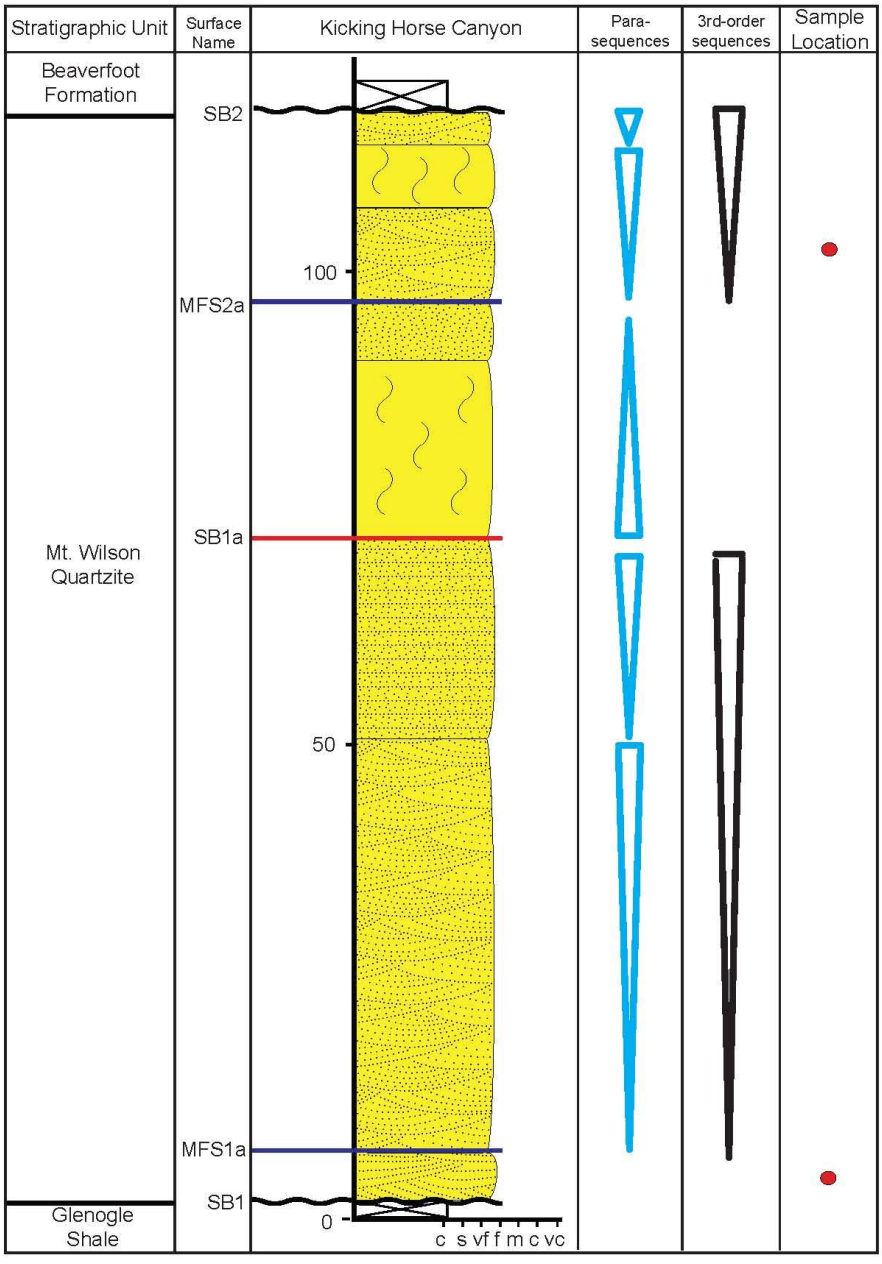
Stratigraphic Unit
Surface Name
Kicking Horse Canyon
Para-sequences
3rd-order sequences
Sample Location
Beaverfoot Formation
SB2
100
MFS2a
SB1a
Mt. Wilson Quartzite
50
MFS1a
SB1
Glenogle Shale
0
c s vf f m c vc

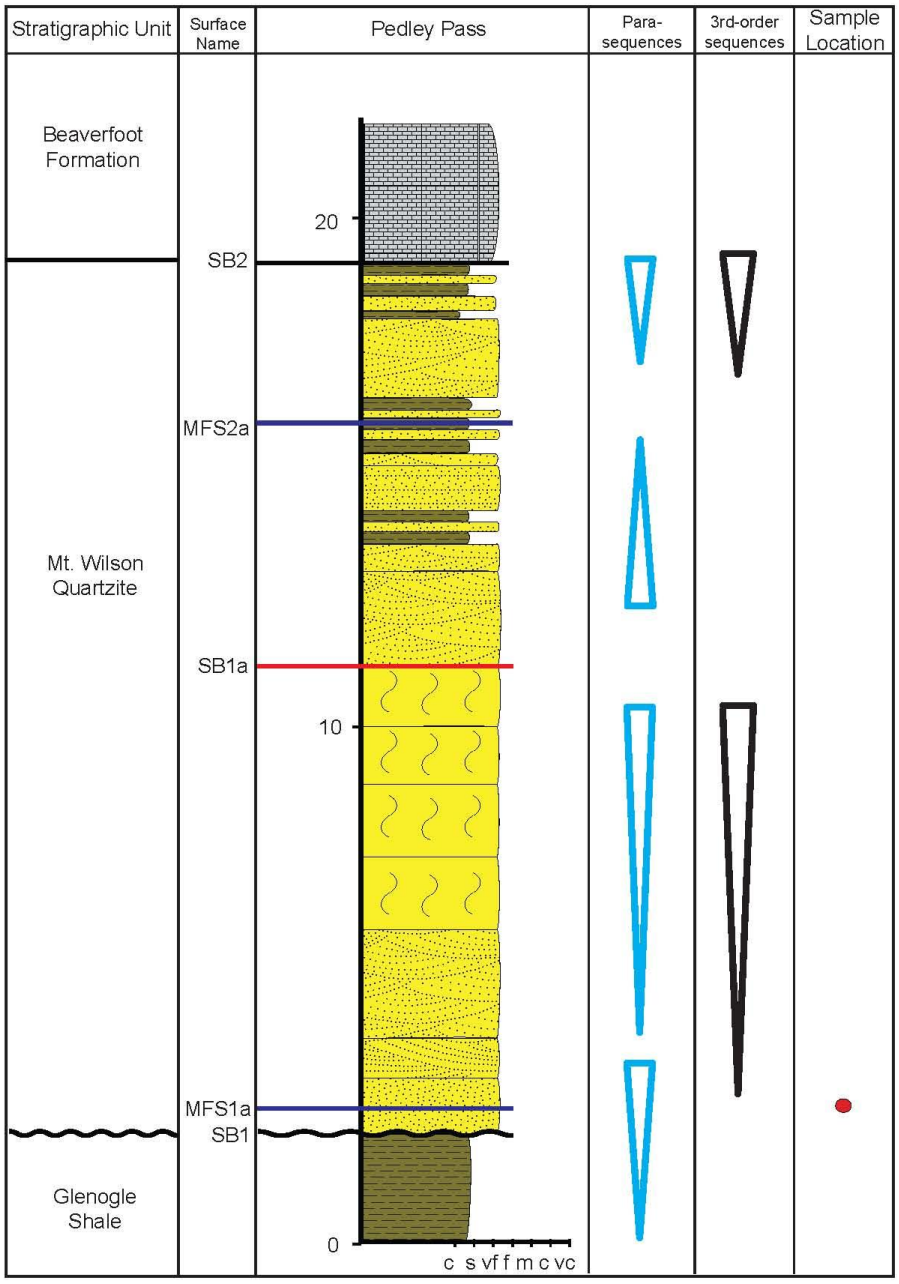
Stratigraphic Unit
Surface Name
Pedley Pass
Para-sequences
3rd-order sequences
Sample Location
Beaverfoot Formation
Mt. Wilson Quartzite
Glenogle Shale
SB2
MFS2a
SB1a
MFS1a
SB1
20
10
0
c s vf f m c vc

APPENDIX C

DATA TABLES

sample name	238U 206Pb	1 sigma % error	207Pb 206Pb	1 sigma % error	*Th U*	206/238 age	1 sigma abs err	207/206 age	1 sigma abs err
< 10 % discordant									
MM1_859	2.970	2.85%	0.11542	1.31%	*0.40*	1870.6	46.1	1886.5	23.4
MM1_867	1.950	1.50%	0.18443	0.67%	*0.40*	2668.5	32.6	2693.1	11.0
MM1_860	2.157	2.49%	0.17402	0.81%	*0.40*	2455.0	50.6	2596.7	13.4
MM1_865	3.358	3.75%	0.11270	1.11%	*0.40*	1680.5	55.2	1843.4	19.9
MM1_868	2.527	1.94%	0.12887	0.82%	*0.40*	2149.2	35.3	2082.6	14.4
MM1_871	3.046	1.58%	0.11209	0.76%	*0.40*	1830.2	25.1	1833.6	13.7
MM1_873	2.950	1.27%	0.11829	0.69%	*0.40*	1881.6	20.7	1930.5	12.4
MM1_869	2.954	1.58%	0.11761	0.80%	*0.40*	1879.7	25.7	1920.2	14.3
MM1_862	2.935	0.68%	0.11861	0.67%	*0.40*	1890.3	11.1	1935.4	12.0
MM1_846	1.945	1.83%	0.17459	0.76%	*0.40*	2673.9	40.0	2602.1	12.6
MM1_839	3.092	1.32%	0.11251	0.80%	*0.40*	1806.5	20.7	1840.4	14.4
MM1_848	2.905	1.16%	0.11926	0.76%	*0.40*	1906.8	19.2	1945.2	13.5
MM1_853	3.091	1.65%	0.11274	0.86%	*0.40*	1807.0	26.0	1844.0	15.5
MM1_855	2.974	0.79%	0.11552	0.71%	*0.40*	1868.8	12.8	1887.9	12.7
MM1_799	2.780	2.06%	0.11749	0.86%	*0.40*	1980.9	35.0	1918.3	15.4
MM1_758	2.937	1.40%	0.11641	0.80%	*0.40*	1889.0	22.8	1901.8	14.2
MM1_761	3.049	1.82%	0.11272	0.92%	*0.40*	1828.5	28.9	1843.8	16.6
MM1_729	5.807	1.25%	0.07359	0.86%	*0.40*	1024.3	11.9	1030.1	17.2
MM1_765	2.929	1.67%	0.11834	0.91%	*0.40*	1893.3	27.3	1931.4	16.2
MM1_589	2.966	0.93%	0.11788	0.63%	*0.40*	1872.8	15.0	1924.4	11.2
MM1_626	2.970	0.89%	0.11737	0.67%	*0.40*	1870.9	14.4	1916.6	12.0
MM1_587	3.137	1.70%	0.11001	0.86%	*0.40*	1783.9	26.4	1799.5	15.6
MM1_538b	2.163	1.21%	0.16716	0.68%	*0.40*	2450.1	24.6	2529.4	11.4
MM1_599	2.830	1.29%	0.11715	0.74%	*0.40*	1950.6	21.7	1913.2	13.2
MM1_535	2.406	1.38%	0.14799	0.70%	*0.40*	2240.6	26.0	2322.8	12.0
MM1_477	3.091	1.40%	0.11364	0.84%	*0.40*	1806.8	22.1	1858.5	15.0
MM1_422	2.066	1.31%	0.17485	0.68%	*0.40*	2544.7	27.5	2604.6	11.3
MM1_393	2.983	1.91%	0.11917	0.84%	*0.40*	1863.6	30.8	1943.8	15.0
MM1_258	1.927	1.18%	0.18773	0.70%	*0.40*	2694.3	26.0	2722.3	11.4
MM1_284	2.851	1.16%	0.11365	0.72%	*0.40*	1938.3	19.5	1858.5	13.0

MM1_324	2.059	1.17%	0.17097	0.69%	*0.40*	2552.0	24.5	2567.2	11.5
MM1_289	2.467	1.45%	0.13858	0.75%	*0.40*	2193.9	26.9	2209.5	12.9
MM1_309	2.907	1.72%	0.12085	0.83%	*0.40*	1905.7	28.3	1968.8	14.7
MM1_322	2.950	1.84%	0.11263	0.92%	*0.40*	1881.8	30.0	1842.3	16.6
MM1_184b	3.207	1.53%	0.11112	0.74%	*0.40*	1749.8	23.4	1817.9	13.3
MM1_164	2.731	1.79%	0.11785	0.82%	*0.40*	2011.6	30.9	1923.9	14.6
MM1_138	2.710	2.45%	0.12200	0.90%	*0.40*	2024.8	42.4	1985.7	16.0
MM1_144	2.982	2.00%	0.11223	0.87%	*0.40*	1864.1	32.3	1835.9	15.7
MM1_112	5.789	1.64%	0.07335	0.95%	*0.40*	1027.2	15.6	1023.5	19.0
MM1_56	2.822	2.09%	0.11169	0.88%	*0.40*	1955.4	35.2	1827.2	15.8
MM1_43	2.798	1.81%	0.11741	0.82%	*0.40*	1969.6	30.7	1917.1	14.7
MM1_21	2.984	1.53%	0.11253	0.70%	*0.40*	1863.2	24.7	1840.6	12.6
MM1_36	2.046	1.80%	0.16740	0.71%	*0.40*	2565.0	38.0	2531.9	11.9
MM1_60	3.438	1.75%	0.10161	0.81%	*0.40*	1646.0	25.4	1653.8	15.0
MM1_61	3.052	1.87%	0.11004	0.71%	*0.40*	1826.8	29.7	1800.1	12.8
MM1_73	2.514	2.76%	0.12629	0.90%	*0.40*	2159.0	50.5	2047.0	15.8
MM1_101b	2.750	2.23%	0.12617	0.84%	*0.40*	1999.6	38.2	2045.3	14.7
MM1_141	3.095	1.99%	0.10991	0.80%	*0.40*	1804.7	31.2	1797.9	14.5
MM1_158	2.868	1.89%	0.11886	0.72%	*0.40*	1928.6	31.4	1939.1	12.9
MM1_202	3.038	2.29%	0.11169	0.83%	*0.40*	1834.3	36.4	1827.0	15.0
MM1_204	2.660	2.18%	0.12640	0.79%	*0.40*	2057.2	38.3	2048.6	13.8
MM1_214	3.092	2.10%	0.11302	0.75%	*0.40*	1806.2	33.0	1848.5	13.5
MM1_194	2.882	2.13%	0.11689	0.83%	*0.40*	1920.3	35.2	1909.2	14.8
MM1_251	2.899	1.93%	0.11591	0.75%	*0.40*	1910.6	31.8	1894.1	13.4
MM1_334	2.795	1.94%	0.11883	0.84%	*0.40*	1971.7	32.8	1938.7	14.9
MM1_335	2.900	2.03%	0.11749	0.78%	*0.40*	1910.1	33.5	1918.4	13.9
MM1_371	1.866	2.11%	0.18422	0.75%	*0.40*	2766.9	47.4	2691.2	12.3
MM1_357	3.067	1.88%	0.11362	0.76%	*0.40*	1819.0	29.7	1858.1	13.6
MM1_367	3.149	1.85%	0.10952	0.71%	*0.40*	1777.7	28.6	1791.5	12.8
MM1_368	2.007	1.76%	0.17630	0.68%	*0.40*	2606.2	37.6	2618.4	11.2
MM1_374	2.998	1.77%	0.11448	0.75%	*0.40*	1855.9	28.5	1871.8	13.4
MM1_502	3.164	1.73%	0.11238	0.72%	*0.40*	1770.3	26.7	1838.3	12.9
MM1_474	2.639	1.88%	0.12823	0.76%	*0.40*	2071.4	33.2	2073.9	13.4
MM1_508	3.040	1.98%	0.11160	0.77%	*0.40*	1833.1	31.6	1825.7	14.0
MM1_549	2.637	1.53%	0.12853	0.77%	*0.40*	2072.3	27.1	2078.0	13.5
MM1_544	2.818	1.17%	0.11640	0.72%	*0.40*	1958.0	19.8	1901.6	12.9
MM1_536	1.756	1.38%	0.20531	0.70%	*0.40*	2905.1	32.1	2868.9	11.3
MM1_530	2.976	1.34%	0.11290	0.78%	*0.40*	1867.7	21.8	1846.6	14.0
MM1_604	2.701	2.54%	0.11684	0.97%	*0.40*	2030.6	44.0	1908.4	17.3
MM1_706	2.993	1.46%	0.11801	0.81%	*0.40*	1858.3	23.4	1926.4	14.4

MM1_797	2.938	0.92%	0.11440	0.69%	*0.40*	1888.3	15.0	1870.5	12.4
MM1_841	2.868	2.59%	0.11795	0.97%	*0.40*	1928.3	43.0	1925.3	17.3
MM1_619	3.051	1.13%	0.11393	0.72%	*0.40*	1827.5	18.0	1863.0	13.0
MM1_639	2.793	0.94%	0.11862	0.70%	*0.40*	1972.9	16.0	1935.6	12.5
MM1_625	1.909	1.81%	0.18196	0.80%	*0.40*	2716.0	40.0	2670.8	13.1
MM1_642	2.675	3.81%	0.12928	1.21%	*0.40*	2047.5	66.5	2088.2	21.1
MM1_725	2.922	2.25%	0.11101	0.85%	*0.40*	1897.6	36.9	1815.9	15.3
MM1_711	2.882	1.76%	0.11268	0.76%	*0.40*	1920.2	29.2	1843.1	13.7
MM1_709	2.938	1.67%	0.11155	0.73%	*0.40*	1888.5	27.3	1824.8	13.3
MM1_800	2.909	1.79%	0.11156	0.78%	*0.40*	1905.0	29.5	1824.9	14.1
MM1_806	2.983	1.86%	0.11234	0.78%	*0.40*	1863.9	30.1	1837.7	14.1
MM1_858	3.080	2.40%	0.11253	0.89%	*0.40*	1812.3	37.8	1840.7	16.0
MM1_813	2.494	2.11%	0.12762	0.80%	*0.40*	2173.7	38.9	2065.5	14.0
MM1_784	2.857	9.44%	0.11689	1.07%	*0.40*	1934.7	155.9	1909.1	19.1
MM1_702	2.944	9.11%	0.11250	0.97%	*0.40*	1884.8	147.3	1840.1	17.4
MM1_722	3.121	8.85%	0.11383	0.71%	*0.40*	1791.9	136.9	1861.4	12.7
MM1_716	3.182	8.87%	0.11316	0.75%	*0.40*	1761.6	135.3	1850.7	13.6
MM1_690	3.077	8.94%	0.11159	0.81%	*0.40*	1814.3	139.9	1825.4	14.7
MM1_644	3.106	8.87%	0.11833	0.77%	*0.40*	1799.5	137.8	1931.1	13.7
MM1_627	2.755	9.00%	0.12736	0.76%	*0.40*	1996.0	152.6	2061.9	13.4
MM1_523	3.173	8.81%	0.11362	0.69%	*0.40*	1766.1	134.7	1858.1	12.4
MM1_481	3.033	9.00%	0.11245	0.96%	*0.40*	1837.0	142.3	1839.4	17.2
MM1_528	2.984	9.03%	0.11020	0.94%	*0.40*	1863.3	144.5	1802.7	17.1
MM1_406	3.158	3.75%	0.11436	1.47%	*0.40*	1773.4	57.8	1869.9	26.3
MM1_455	2.567	1.99%	0.12888	0.68%	*0.40*	2121.0	35.9	2082.7	11.9
MM1_495	2.158	2.17%	0.14632	0.72%	*0.40*	2454.2	44.2	2303.4	12.3
MM1_484	2.947	2.24%	0.11475	0.78%	*0.40*	1883.6	36.4	1876.0	13.9
MM1_376	3.018	2.99%	0.11293	0.95%	*0.40*	1844.9	47.8	1847.1	17.1
MM1_351	2.855	2.91%	0.11046	1.00%	*0.39*	1935.8	48.5	1807.0	18.0
MM1_282	1.893	2.22%	0.19402	0.69%	*0.39*	2733.8	49.3	2776.6	11.2
MM1_252	2.938	2.22%	0.11460	0.80%	*0.40*	1888.6	36.2	1873.6	14.4
MM1_209	2.893	1.94%	0.11776	0.73%	*0.34*	1913.7	32.1	1922.5	13.0
MM1_108	3.118	4.31%	0.11317	0.92%	*0.35*	1793.5	67.1	1850.9	16.6
MM1_124	3.012	5.81%	0.11542	1.11%	*0.36*	1848.3	92.7	1886.5	19.8
MM1_70	2.764	4.31%	0.12832	0.82%	*0.36*	1990.7	73.4	2075.0	14.4
MM1_9	2.687	4.13%	0.11995	0.95%	*0.20*	2039.3	71.9	1955.4	16.8

sample name	238U 206Pb	1 sigma % error	207Pb 206Pb	1 sigma % error	*Th U*	206/238 age	1 sigma abs err	207/206 age	1 sigma abs err
< 10 % discordant									
MM2_247	2.893	1.65%	0.11284	0.93%	*0.37*	1914.1	27.3	1845.7	16.8
MM2_248	2.815	1.19%	0.11825	0.79%	*0.37*	1959.4	20.1	1929.9	14.1
MM2_244	2.941	1.84%	0.11260	0.94%	*0.37*	1887.0	30.0	1841.8	17.0
MM2_257	1.722	1.55%	0.21837	0.73%	*0.37*	2951.5	36.6	2968.7	11.7
MM2_267	2.549	2.29%	0.13090	0.99%	*0.37*	2133.3	41.5	2110.1	17.2
MM2_274	2.808	2.38%	0.11688	0.95%	*0.40*	1963.7	40.2	1909.0	17.0
MM2_278	2.907	2.43%	0.11418	1.02%	*0.40*	1906.0	40.0	1867.0	18.3
MM2_279	3.066	1.67%	0.11167	0.87%	*0.40*	1819.7	26.4	1826.7	15.7
MM2_271	2.898	1.42%	0.11803	0.80%	*0.40*	1910.9	23.4	1926.6	14.3
MM2_272	1.813	2.02%	0.18605	0.82%	*0.40*	2831.2	46.1	2707.6	13.5
MM2_262	2.943	1.22%	0.11622	0.72%	*0.40*	1885.6	19.9	1898.8	13.0
MM2_216	2.192	1.32%	0.15006	0.76%	*0.40*	2422.9	26.5	2346.6	12.9
MM2_184a	2.858	1.57%	0.11676	0.81%	*0.40*	1934.4	26.2	1907.2	14.4
MM2_200	2.804	1.21%	0.12790	0.73%	*0.40*	1966.4	20.5	2069.4	12.9
MM2_202	2.838	1.53%	0.11739	0.85%	*0.40*	1946.1	25.6	1916.9	15.1
MM2_208	2.968	2.72%	0.11473	1.15%	*0.40*	1871.9	44.1	1875.7	20.5
MM2_238	3.040	1.74%	0.11267	0.85%	*0.40*	1833.1	27.7	1842.9	15.3
MM2_259	2.668	2.08%	0.12106	0.95%	*0.40*	2052.0	36.5	1971.8	16.9
MM2_242	2.863	1.56%	0.11659	0.84%	*0.40*	1931.0	25.9	1904.6	15.0
MM2_232	2.655	2.42%	0.12466	1.00%	*0.40*	2060.8	42.6	2024.0	17.6
MM2_212	3.079	0.94%	0.11033	0.73%	*0.40*	1813.1	14.8	1804.8	13.2
MM2_139	2.716	1.03%	0.12939	0.74%	*0.40*	2020.8	17.8	2089.7	12.9
MM2_149	2.656	0.93%	0.12838	0.71%	*0.40*	2059.7	16.4	2076.0	12.4
MM2_147	3.027	1.23%	0.11176	0.83%	*0.40*	1839.9	19.6	1828.2	14.9
MM2_155	3.044	3.20%	0.11233	1.17%	*0.40*	1831.3	50.9	1837.4	21.0
MM2_178	2.284	1.55%	0.14592	0.79%	*0.40*	2340.7	30.4	2298.6	13.4
MM2_180	2.857	0.88%	0.11831	0.75%	*0.40*	1934.6	14.8	1930.8	13.4
MM2_193	2.074	1.42%	0.16903	0.69%	*0.40*	2536.5	29.7	2548.1	11.5
MM2_160	2.038	1.58%	0.17719	0.74%	*0.40*	2573.9	33.5	2626.8	12.2
MM2_190	2.792	2.08%	0.11724	0.85%	*0.40*	1973.4	35.3	1914.5	15.2
MM2_187	2.972	1.55%	0.11435	0.74%	*0.40*	1869.5	25.1	1869.6	13.3
MM2_185	2.750	2.09%	0.11733	0.88%	*0.40*	1999.7	35.9	1915.9	15.7
MM2_182	2.821	2.34%	0.11814	0.95%	*0.40*	1955.7	39.4	1928.3	16.9
MM2_163	3.064	1.60%	0.11217	0.78%	*0.40*	1820.5	25.3	1834.9	14.0

MM2_152	2.864	1.84%	0.11474	0.86%	*0.40*	1930.8	30.6	1875.9	15.5
MM2_143	2.882	2.51%	0.11225	1.02%	*0.40*	1920.1	41.5	1836.1	18.3
MM2_130	2.865	2.49%	0.11877	0.81%	*0.40*	1929.8	41.3	1937.8	14.5
MM2_128	3.065	2.40%	0.11229	0.77%	*0.40*	1820.4	37.9	1836.8	13.8
MM2_127	2.940	2.97%	0.11149	0.96%	*0.40*	1887.4	48.4	1823.8	17.4
MM2_103	2.944	3.40%	0.11356	1.11%	*0.40*	1885.3	55.3	1857.2	19.9
MM2_98	2.394	3.30%	0.12819	1.05%	*0.40*	2250.0	62.4	2073.3	18.3
MM2_78	2.978	3.45%	0.11462	1.24%	*0.40*	1866.3	55.7	1873.9	22.2
MM2_52	1.994	3.28%	0.18193	0.98%	*0.40*	2620.1	70.2	2670.6	16.2
MM2_47	3.341	2.50%	0.11205	0.74%	*0.40*	1688.1	37.0	1832.9	13.3
MM2_48	2.928	2.53%	0.11750	0.87%	*0.40*	1893.8	41.4	1918.6	15.4
MM2_22b	2.639	3.30%	0.12836	0.97%	*0.40*	2071.6	58.2	2075.6	17.0
MM2_22a	2.696	0.97%	0.12939	0.76%	*0.40*	2033.8	17.0	2089.7	13.4
MM2_11	3.012	2.27%	0.11376	0.93%	*0.40*	1848.0	36.4	1860.3	16.6
MM2_10	3.068	1.23%	0.11141	0.79%	*0.40*	1818.6	19.4	1822.5	14.3
MM2_6	3.000	1.17%	0.11435	0.80%	*0.40*	1854.7	18.8	1869.6	14.4
MM2_18	2.890	1.08%	0.11617	0.76%	*0.40*	1915.7	17.8	1898.1	13.6
MM2_20	2.891	1.26%	0.11612	0.85%	*0.40*	1915.0	20.8	1897.4	15.1
MM2_30	2.320	0.97%	0.14792	0.73%	*0.40*	2310.6	18.8	2322.1	12.4
MM2_39b	2.913	1.04%	0.11892	0.81%	*0.40*	1902.2	17.1	1940.0	14.4
MM2_58	3.113	1.16%	0.11130	0.86%	*0.40*	1795.7	18.1	1820.8	15.5
MM2_55	3.077	0.92%	0.11210	0.75%	*0.40*	1813.8	14.5	1833.7	13.5
MM2_45	3.047	1.09%	0.11307	0.80%	*0.40*	1829.8	17.3	1849.3	14.4
MM2_53	3.050	1.45%	0.11334	0.85%	*0.40*	1828.0	23.1	1853.7	15.3
MM2_60	2.022	1.05%	0.17659	0.71%	*0.40*	2590.1	22.4	2621.1	11.7
MM2_62	2.923	1.04%	0.11737	0.74%	*0.40*	1896.6	17.0	1916.5	13.2
MM2_109	2.890	1.69%	0.11657	0.89%	*0.40*	1915.4	27.9	1904.2	15.9
MM2_80	3.056	1.28%	0.11337	0.85%	*0.40*	1825.0	20.3	1854.1	15.4
MM2_90	2.602	1.65%	0.12798	0.88%	*0.40*	2096.7	29.5	2070.4	15.5
MM2_97	2.956	1.97%	0.11450	0.98%	*0.40*	1878.5	32.1	1872.0	17.6
MM2_105	2.705	1.86%	0.13009	1.05%	*0.40*	2028.1	32.3	2099.2	18.4
MM2_102	3.016	1.63%	0.11066	0.88%	*0.40*	1846.1	26.1	1810.3	15.9
MM2_107	2.661	1.04%	0.12597	0.77%	*0.40*	2056.6	18.3	2042.5	13.5
MM2_101	3.050	1.48%	0.11152	0.88%	*0.40*	1828.2	23.5	1824.3	15.8
MM2_123	3.052	0.91%	0.11248	0.76%	*0.40*	1827.0	14.5	1839.8	13.7
MM2_154	2.910	2.00%	0.11354	1.04%	*0.40*	1904.2	32.9	1856.8	18.8
MM2_177	2.608	1.17%	0.12893	0.77%	*0.40*	2092.4	20.9	2083.4	13.5
MM2_172	2.860	1.18%	0.11833	0.80%	*0.40*	1932.8	19.7	1931.2	14.3
MM2_170	2.887	1.11%	0.11880	0.70%	*0.40*	1917.5	18.3	1938.2	12.5
MM2_138	2.825	1.06%	0.11729	0.71%	*0.40*	1953.4	17.8	1915.3	12.7

MM2_133	2.925	2.27%	0.11306	1.03%	*0.40*	1895.8	37.3	1849.1	18.5
MM2_135	2.592	1.10%	0.14344	0.74%	*0.40*	2103.4	19.7	2269.1	12.8
MM2_131	2.762	2.16%	0.11761	0.96%	*0.40*	1992.2	36.9	1920.3	17.2
MM2_124	2.543	1.02%	0.13207	0.78%	*0.40*	2138.0	18.6	2125.7	13.5
MM2_121	3.042	1.25%	0.11127	0.84%	*0.40*	1832.2	19.9	1820.3	15.1
MM2_104	2.930	2.83%	0.11248	1.08%	*0.40*	1892.8	46.2	1839.9	19.4
MM2_99	2.468	2.61%	0.13022	1.11%	*0.40*	2192.8	48.4	2100.9	19.3
MM2_51a	2.888	0.94%	0.11765	0.73%	*0.40*	1916.8	15.6	1920.9	13.1
MM2_59	2.012	0.96%	0.17268	0.72%	*0.40*	2601.1	20.4	2583.8	12.0
MM2_37	1.708	1.16%	0.22389	0.72%	*0.40*	2971.0	27.6	3008.8	11.6
MM2_26	2.422	1.22%	0.14849	0.76%	*0.40*	2227.7	22.9	2328.6	13.0
MM2_8	2.944	1.04%	0.11532	0.75%	*0.40*	1885.1	16.9	1884.8	13.5
MM2_23	2.882	1.73%	0.13196	0.97%	*0.40*	1920.0	28.6	2124.2	16.9
MM2_25	3.021	1.60%	0.11268	0.86%	*0.40*	1843.6	25.7	1843.0	15.5
MM2_27	3.091	1.02%	0.11091	0.71%	*0.40*	1806.8	16.0	1814.4	12.8
MM2_42	2.887	1.21%	0.11149	0.80%	*0.40*	1917.3	20.1	1823.8	14.5
MM2_74	3.010	1.32%	0.11088	0.81%	*0.40*	1849.1	21.3	1813.8	14.6
MM2_151	3.005	1.02%	0.11131	0.70%	*0.40*	1852.0	16.4	1820.9	12.7
MM2_115	2.971	2.07%	0.11213	0.94%	*0.40*	1870.5	33.5	1834.2	16.8
MM2_110	2.305	0.95%	0.14818	0.70%	*0.40*	2322.6	18.5	2325.0	11.9
MM2_111	2.860	1.22%	0.11853	0.79%	*0.40*	1932.9	20.3	1934.1	14.1
MM2_86	2.767	1.72%	0.11784	0.89%	*0.40*	1989.0	29.3	1923.7	15.9
MM2_94	2.927	2.24%	0.11596	1.04%	*0.40*	1894.7	36.6	1894.8	18.5
MM2_85	2.308	1.57%	0.15855	0.80%	*0.40*	2320.1	30.6	2440.2	13.6
MM2_77	2.612	1.16%	0.12716	0.89%	*0.40*	2089.8	20.7	2059.1	15.7
MM2_66	2.971	1.99%	0.11326	1.06%	*0.40*	1870.3	32.2	1852.3	19.1
MM2_46	2.874	1.61%	0.11514	1.00%	*0.39*	1924.7	26.8	1882.1	18.0
MM2_49	2.892	1.61%	0.11659	0.99%	*0.40*	1914.6	26.6	1904.6	17.7
MM2_41	2.896	1.79%	0.11260	1.02%	*0.34*	1912.0	29.5	1841.8	18.3
MM2_36	1.884	1.52%	0.18812	0.90%	*0.35*	2744.5	33.8	2725.8	14.7
MM2_32	3.008	1.98%	0.11412	1.07%	*0.36*	1850.3	31.8	1866.0	19.3
MM2_24	3.094	1.64%	0.11307	0.99%	*0.36*	1805.4	25.7	1849.4	17.9
MM2_13	2.914	1.20%	0.11914	0.89%	*0.29*	1901.8	19.7	1943.3	15.9
MM2_2	3.017	1.58%	0.11123	0.98%	*0.20*	1845.2	25.3	1819.7	17.7

sample name	238U 206Pb	1 sigma % error	207Pb 206Pb	1 sigma % error	*Th U*	206/238 age	1 sigma abs err	207/206 age	1 sigma abs err
< 10 % discordant									
MM3_272	2.859	2.54%	0.11768	1.00%	*0.37*	1933.5	42.3	1921.3	17.7
MM3_254	3.025	2.26%	0.11372	0.88%	*0.37*	1841.3	36.1	1859.7	15.7
MM3_244	3.165	1.85%	0.11295	0.81%	*0.37*	1770.1	28.6	1847.5	14.6
MM3_256	3.058	2.71%	0.11377	0.90%	*0.37*	1823.8	42.9	1860.5	16.2
MM3_266	3.193	1.74%	0.11252	0.76%	*0.40*	1756.6	26.8	1840.5	13.6
MM3_276	2.732	1.83%	0.12795	0.76%	*0.40*	2010.9	31.6	2070.0	13.3
MM3_290	2.857	1.78%	0.12222	0.74%	*0.40*	1934.6	29.6	1988.8	13.1
MM3_297	5.955	1.68%	0.07449	0.84%	*0.40*	1000.7	15.6	1054.7	16.9
MM3_284	2.379	1.76%	0.15121	0.71%	*0.40*	2262.0	33.6	2359.6	12.1
MM3_263	2.888	2.32%	0.11335	1.01%	*0.40*	1916.5	38.3	1853.8	18.1
MM3_255	2.582	1.40%	0.14446	0.76%	*0.40*	2110.1	25.1	2281.4	13.1
MM3_252	3.068	2.72%	0.11218	1.03%	*0.40*	1818.9	42.9	1835.0	18.6
MM3_260	2.962	1.94%	0.11321	0.99%	*0.40*	1875.3	31.5	1851.5	17.9
MM3_271	3.047	2.94%	0.10992	1.02%	*0.40*	1829.4	46.6	1798.0	18.4
MM3_277	1.179	2.67%	0.43164	0.76%	*0.40*	3959.6	78.4	4023.1	11.4
MM3_294	3.068	1.30%	0.11098	0.76%	*0.40*	1818.8	20.5	1815.6	13.8
MM3_308	3.116	1.54%	0.11340	0.85%	*0.40*	1794.4	24.1	1854.6	15.2
MM3_316	3.116	1.81%	0.11464	0.94%	*0.40*	1794.5	28.3	1874.3	16.9
MM3_312	2.921	1.97%	0.11109	0.90%	*0.40*	1897.7	32.3	1817.3	16.2
MM3_305	2.823	2.10%	0.11742	0.97%	*0.40*	1954.8	35.3	1917.4	17.2
MM3_306	2.589	2.12%	0.12871	0.91%	*0.40*	2105.5	38.0	2080.4	16.0
MM3_311	3.135	1.50%	0.11068	0.82%	*0.40*	1784.9	23.3	1810.6	14.9
MM3_307	2.687	1.24%	0.12777	0.77%	*0.40*	2039.8	21.7	2067.5	13.6
MM3_314	2.011	1.05%	0.18620	0.69%	*0.40*	2602.3	22.4	2708.9	11.3
MM3_299	2.915	1.25%	0.11873	0.77%	*0.40*	1901.4	20.6	1937.2	13.7
MM3_292	2.901	1.08%	0.11803	0.75%	*0.40*	1909.1	17.8	1926.6	13.4
MM3_278	1.928	0.99%	0.18408	0.69%	*0.40*	2693.4	21.7	2690.0	11.3
MM3_261	5.576	2.34%	0.07511	1.55%	*0.40*	1063.4	22.9	1071.3	30.9
MM3_257	2.014	1.43%	0.18451	0.77%	*0.40*	2599.2	30.5	2693.8	12.6
MM3_243	3.023	1.01%	0.11749	0.76%	*0.40*	1842.3	16.2	1918.4	13.5
MM3_231	2.954	1.75%	0.11719	0.76%	*0.40*	1879.4	28.5	1913.8	13.7
MM3_214	2.977	2.10%	0.11653	0.80%	*0.40*	1866.9	34.0	1903.6	14.3
MM3_206	2.762	1.93%	0.12568	0.78%	*0.40*	1992.2	33.1	2038.5	13.8
MM3_174	3.029	1.88%	0.11744	0.81%	*0.40*	1838.9	30.0	1917.6	14.4
MM3_183	2.915	1.81%	0.11765	0.80%	*0.40*	1901.2	29.7	1920.8	14.3

MM3_180	3.022	1.91%	0.11381	0.86%	*0.40*	1842.9	30.5	1861.2	15.5
MM3_200	2.005	1.68%	0.18658	0.69%	*0.40*	2608.0	35.8	2712.3	11.4
MM3_208	2.710	1.60%	0.12766	0.67%	*0.40*	2024.7	27.7	2066.0	11.9
MM3_226	1.816	1.70%	0.20923	0.68%	*0.40*	2827.5	38.8	2899.6	10.9
MM3_233	2.393	1.72%	0.14638	0.74%	*0.40*	2250.7	32.6	2304.1	12.6
MM3_239	2.953	2.01%	0.11220	0.82%	*0.40*	1880.1	32.7	1835.3	14.8
MM3_247	2.765	1.50%	0.12477	0.75%	*0.40*	1990.2	25.6	2025.5	13.1
MM3_232	2.902	1.55%	0.11417	0.74%	*0.40*	1908.7	25.6	1866.8	13.2
MM3_203	3.090	2.40%	0.11128	1.01%	*0.40*	1807.5	37.7	1820.5	18.3
MM3_187	2.980	1.99%	0.11612	0.83%	*0.40*	1865.5	32.2	1897.4	14.8
MM3_167	2.896	1.17%	0.11759	0.77%	*0.40*	1912.0	19.4	1920.0	13.8
MM3_143	2.917	0.84%	0.11854	0.67%	*0.40*	1900.3	13.8	1934.4	12.0
MM3_171	3.034	1.88%	0.11221	0.93%	*0.40*	1836.2	30.0	1835.5	16.8
MM3_195	2.645	1.95%	0.12730	0.88%	*0.40*	2067.3	34.4	2061.0	15.5
MM3_240	5.971	0.91%	0.07342	0.74%	*0.40*	998.3	8.4	1025.5	14.9
MM3_227	2.697	1.63%	0.12946	0.81%	*0.40*	2032.8	28.3	2090.7	14.1
MM3_218	2.638	1.56%	0.12833	0.78%	*0.40*	2072.1	27.5	2075.2	13.6
MM3_230	2.674	1.71%	0.12942	0.76%	*0.40*	2047.9	29.9	2090.1	13.3
MM3_238	3.102	1.34%	0.11145	0.75%	*0.40*	1801.5	21.0	1823.3	13.5
MM3_262	2.990	1.28%	0.11595	0.74%	*0.40*	1860.2	20.6	1894.7	13.3
MM3_274	2.064	1.61%	0.18088	0.72%	*0.40*	2546.7	33.8	2661.0	11.8
MM3_285	3.149	1.29%	0.11245	0.73%	*0.40*	1777.6	20.1	1839.3	13.2
MM3_295	3.034	1.92%	0.11065	0.83%	*0.40*	1836.5	30.6	1810.1	14.9
MM3_298	2.666	1.75%	0.12886	0.79%	*0.40*	2053.3	30.8	2082.5	13.9
MM3_296	2.892	3.32%	0.11765	1.23%	*0.40*	1914.6	54.7	1920.8	22.0
MM3_280	2.876	2.60%	0.11885	1.10%	*0.40*	1923.5	43.1	1939.1	19.5
MM3_264	2.911	2.98%	0.11693	0.96%	*0.40*	1903.7	49.0	1909.8	17.2
MM3_44	2.543	2.65%	0.12787	0.86%	*0.40*	2137.7	48.1	2069.0	15.1
MM3_37	2.819	2.98%	0.12226	1.10%	*0.40*	1957.3	50.1	1989.5	19.5
MM3_159	3.071	0.80%	0.11470	0.71%	*0.40*	1817.0	12.7	1875.2	12.7
MM3_164	3.005	1.16%	0.12124	0.82%	*0.40*	1852.0	18.6	1974.5	14.5
MM3_163	2.650	1.79%	0.12696	0.86%	*0.40*	2064.0	31.5	2056.3	15.1
MM3_124	2.866	2.08%	0.11945	0.97%	*0.40*	1929.7	34.6	1948.0	17.2
MM3_101	3.003	1.00%	0.11739	0.73%	*0.40*	1852.7	16.1	1916.8	13.0
MM3_55	2.923	2.21%	0.11734	0.89%	*0.40*	1897.0	36.3	1916.1	15.9
MM3_69	2.937	1.66%	0.11716	0.79%	*0.40*	1888.8	27.1	1913.3	14.0
MM3_103	2.965	1.92%	0.11530	0.87%	*0.40*	1873.4	31.1	1884.6	15.7
MM3_116	3.153	1.38%	0.11310	0.71%	*0.40*	1776.1	21.4	1849.8	12.8
MM3_110	2.925	3.27%	0.11319	1.18%	*0.40*	1895.8	53.5	1851.3	21.1
MM3_145	2.944	1.35%	0.11783	0.71%	*0.40*	1884.9	22.0	1923.6	12.7

MM3_160	2.926	1.51%	0.12097	0.71%	*0.40*	1895.2	24.7	1970.7	12.7
MM3_155	2.974	2.00%	0.11416	0.83%	*0.40*	1868.8	32.4	1866.7	14.9
MM3_146	3.090	1.89%	0.11181	0.83%	*0.40*	1807.6	29.7	1829.0	15.0
MM3_150	1.977	2.63%	0.18591	0.82%	*0.40*	2638.5	56.6	2706.3	13.5
MM3_154	2.677	2.23%	0.12891	0.78%	*0.40*	2046.2	39.0	2083.2	13.6
MM3_153	2.916	2.97%	0.11077	1.12%	*0.40*	1900.8	48.8	1812.0	20.2
MM3_141	1.957	2.88%	0.17722	0.95%	*0.40*	2660.4	62.4	2627.0	15.8
MM3_142	1.884	2.12%	0.18800	0.80%	*0.40*	2745.2	47.2	2724.7	13.2
MM3_170	2.135	2.19%	0.16988	0.77%	*0.40*	2476.9	44.9	2556.5	12.9
MM3_152	3.039	2.05%	0.11243	0.89%	*0.40*	1833.7	32.6	1839.1	16.0
MM3_129	2.883	1.45%	0.11685	0.78%	*0.40*	1919.5	24.1	1908.7	14.0
MM3_132	2.986	1.04%	0.11827	0.71%	*0.40*	1862.2	16.8	1930.2	12.7
MM3_136	2.696	0.89%	0.12902	0.67%	*0.40*	2033.5	15.5	2084.7	11.8
MM3_115	2.284	2.19%	0.14285	0.81%	*0.40*	2341.3	42.9	2262.0	13.9
MM3_102	2.540	1.95%	0.12931	0.85%	*0.40*	2140.2	35.4	2088.6	14.9
MM3_91	2.106	2.85%	0.16336	0.87%	*0.40*	2505.1	59.0	2490.8	14.6
MM3_81	2.962	1.85%	0.11322	0.77%	*0.40*	1875.2	30.0	1851.8	13.9
MM3_71	2.127	2.25%	0.17242	0.77%	*0.40*	2483.9	46.3	2581.3	12.8
MM3_79	2.081	1.81%	0.17459	0.68%	*0.40*	2529.2	37.7	2602.1	11.3
MM3_56	2.991	1.62%	0.11735	0.68%	*0.40*	1859.5	26.1	1916.3	12.2
MM3_50	2.708	2.99%	0.12818	0.87%	*0.40*	2026.2	51.7	2073.1	15.2
MM3_70	2.916	2.62%	0.11638	0.88%	*0.40*	1900.5	42.9	1901.3	15.8
MM3_76	3.054	2.89%	0.11746	0.88%	*0.40*	1825.8	45.7	1918.0	15.6
MM3_78	3.025	1.85%	0.11828	0.73%	*0.40*	1841.2	29.5	1930.4	13.0
MM3_63	3.035	2.34%	0.11054	0.80%	*0.40*	1835.8	37.3	1808.4	14.5
MM3_52	2.426	2.19%	0.13883	0.72%	*0.39*	2225.2	41.1	2212.7	12.4
MM3_31	2.992	2.66%	0.11884	0.79%	*0.39*	1858.8	42.8	1938.9	14.1
MM3_28	2.671	2.72%	0.12880	0.86%	*0.40*	2050.0	47.5	2081.7	15.1
MM3_10	2.907	3.44%	0.11185	1.23%	*0.34*	1906.1	56.5	1829.8	22.1
MM3_20	3.005	2.53%	0.11799	0.76%	*0.35*	1851.9	40.7	1925.9	13.6
MM3_30	2.792	3.51%	0.11597	1.09%	*0.36*	1973.5	59.5	1895.0	19.5
MM3_29	2.774	2.02%	0.12469	0.69%	*0.36*	1984.6	34.4	2024.5	12.2
MM3_33	3.092	2.05%	0.11138	0.72%	*0.29*	1806.6	32.3	1822.0	13.0
MM3_9	1.942	2.61%	0.17576	0.78%	*0.20*	2677.3	57.0	2613.2	13.0

sample name	238U 206Pb	1 sigma % error	207Pb 206Pb	1 sigma % error	*Th U*	206/238 age	1 sigma abs err	207/206 age	1 sigma abs err
< 10 % discordant									
KHC1_407	2.136	3.22%	0.16566	0.90%	*0.37*	2475.4	65.9	2514.3	15.0
KHC1_388	2.941	3.25%	0.11880	0.90%	*0.37*	1886.9	52.9	1938.2	16.0
KHC1_365	2.866	3.95%	0.11624	1.19%	*0.37*	1929.6	65.6	1899.2	21.2
KHC1_318	3.168	3.39%	0.11219	1.02%	*0.40*	1768.6	52.2	1835.2	18.3
KHC1_278	2.897	3.25%	0.11795	0.95%	*0.40*	1911.6	53.5	1925.4	17.0
KHC1_306	2.720	3.55%	0.13074	0.99%	*0.40*	2018.4	61.3	2107.9	17.3
KHC1_317	2.681	3.26%	0.12944	0.92%	*0.40*	2043.2	56.9	2090.4	16.1
KHC1_316	2.626	3.46%	0.12914	1.00%	*0.40*	2080.3	61.3	2086.3	17.4
KHC1_320	2.787	1.32%	0.12757	0.94%	*0.40*	1976.4	22.4	2064.7	16.6
KHC1_297	1.817	1.09%	0.21465	0.91%	*0.40*	2827.2	24.9	2941.0	14.6
KHC1_398	2.718	1.22%	0.12849	0.97%	*0.40*	2019.9	21.2	2077.5	17.0
KHC1_387	3.136	1.02%	0.11129	0.91%	*0.40*	1784.2	15.9	1820.6	16.4
KHC1_375	3.010	1.24%	0.11793	0.96%	*0.40*	1848.9	19.9	1925.1	17.1
KHC1_361	2.590	2.05%	0.12905	1.07%	*0.40*	2104.9	36.7	2085.1	18.8
KHC1_342	3.108	1.43%	0.11181	0.96%	*0.40*	1798.1	22.4	1829.0	17.2
KHC1_312	3.036	1.32%	0.11789	0.99%	*0.40*	1835.5	21.0	1924.4	17.6
KHC1_310	2.009	0.98%	0.18709	0.88%	*0.40*	2604.6	20.9	2716.8	14.4
KHC1_301	3.170	0.83%	0.11261	0.90%	*0.40*	1767.5	12.8	1842.0	16.2
KHC1_296	2.679	0.85%	0.12852	0.90%	*0.40*	2044.8	14.8	2077.8	15.7
KHC1_281a	2.949	1.48%	0.11684	0.97%	*0.40*	1882.1	24.1	1908.4	17.2
KHC1_282	3.063	0.88%	0.11569	0.89%	*0.40*	1821.2	14.0	1890.7	15.9
KHC1_254	2.455	1.23%	0.14492	0.94%	*0.40*	2202.9	22.9	2286.8	16.1
KHC1_258	3.152	1.42%	0.11227	0.99%	*0.40*	1776.5	22.0	1836.5	17.9
KHC1_253	2.873	1.08%	0.12039	0.93%	*0.40*	1925.3	17.9	1962.0	16.5
KHC1_255	3.000	1.05%	0.11717	0.92%	*0.40*	1854.3	17.0	1913.5	16.4
KHC1_214	3.030	1.27%	0.11966	0.91%	*0.40*	1838.6	20.2	1951.1	16.2
KHC1_229	2.830	1.24%	0.12442	0.89%	*0.40*	1950.7	20.9	2020.5	15.6
KHC1_213	2.990	1.29%	0.11835	0.94%	*0.40*	1859.9	20.9	1931.5	16.7
KHC1_210	3.151	1.17%	0.11385	0.89%	*0.40*	1776.8	18.1	1861.7	16.1
KHC1_145	3.126	1.65%	0.11275	1.03%	*0.40*	1789.2	25.8	1844.2	18.4
KHC1_168	1.998	1.39%	0.18124	0.90%	*0.40*	2615.7	29.8	2664.2	14.9
KHC1_152	3.104	1.50%	0.11109	0.99%	*0.40*	1800.5	23.6	1817.3	17.9
KHC1_118	3.110	1.32%	0.11269	0.91%	*0.40*	1797.2	20.7	1843.2	16.4

KHC1_125	3.122	1.50%	0.11139	0.94%	*0.40*	1791.0	23.4	1822.3	17.0
KHC1_123a	3.117	1.57%	0.11220	1.01%	*0.40*	1793.7	24.5	1835.3	18.1
KHC1_123b	2.864	1.20%	0.11941	0.93%	*0.40*	1930.7	20.0	1947.5	16.6
KHC1_171	2.000	0.99%	0.18122	0.89%	*0.40*	2614.1	21.2	2664.0	14.7
KHC1_162	1.941	1.77%	0.17266	1.01%	*0.40*	2678.6	38.6	2583.6	16.7
KHC1_156	3.008	0.91%	0.11337	0.89%	*0.40*	1850.0	14.6	1854.2	16.1
KHC1_107	2.919	1.30%	0.11696	0.98%	*0.40*	1899.0	21.3	1910.3	17.4
KHC1_102	3.028	1.67%	0.11425	1.05%	*0.40*	1839.4	26.6	1868.2	18.8
KHC1_113	3.138	1.23%	0.11007	0.97%	*0.40*	1783.3	19.1	1800.5	17.5
KHC1_132	3.168	1.13%	0.11351	0.94%	*0.40*	1768.3	17.5	1856.4	16.8
KHC1_101	2.681	1.77%	0.12817	1.05%	*0.40*	2043.4	30.9	2073.1	18.4
KHC1_93	3.075	1.10%	0.11322	0.97%	*0.40*	1815.0	17.4	1851.8	17.5
KHC1_115	3.234	1.15%	0.11041	0.98%	*0.40*	1736.8	17.5	1806.1	17.7
KHC1_104	2.774	0.92%	0.12868	0.89%	*0.40*	1984.5	15.7	2080.0	15.6
KHC1_88	3.231	2.41%	0.11240	1.13%	*0.40*	1738.4	36.7	1838.6	20.2
KHC1_83	2.168	1.02%	0.17420	0.89%	*0.40*	2444.8	20.7	2598.4	14.8
KHC1_74	3.273	0.98%	0.10867	0.94%	*0.40*	1718.8	14.7	1777.2	17.0
KHC1_71	3.178	1.11%	0.11351	0.99%	*0.40*	1763.7	17.1	1856.4	17.8
KHC1_68	3.224	1.67%	0.11301	1.21%	*0.40*	1741.8	25.5	1848.4	21.6
KHC1_39	3.008	2.89%	0.11650	1.20%	*0.40*	1850.4	46.4	1903.2	21.5
KHC1_32	3.524	0.94%	0.10429	0.93%	*0.40*	1610.2	13.4	1701.8	17.0
KHC1_23	2.683	2.68%	0.12798	1.18%	*0.40*	2042.1	46.8	2070.4	20.6
KHC1_15	3.179	1.95%	0.10836	1.02%	*0.40*	1763.3	30.0	1772.0	18.5
KHC1_14	3.049	1.90%	0.11681	1.09%	*0.40*	1828.4	30.2	1908.0	19.5
KHC1_8	3.067	1.58%	0.11275	0.90%	*0.40*	1819.1	24.9	1844.2	16.2
KHC1_16	2.433	2.31%	0.15496	1.11%	*0.40*	2219.5	43.2	2401.4	18.7
KHC1_43	3.043	2.84%	0.11112	1.23%	*0.40*	1831.5	45.2	1817.8	22.2
KHC1_28	2.892	2.45%	0.11348	1.08%	*0.40*	1914.3	40.4	1855.8	19.4
KHC1_13	2.912	3.37%	0.11391	1.28%	*0.40*	1902.8	55.3	1862.7	22.9
KHC1_9	3.185	1.58%	0.11058	0.91%	*0.40*	1760.0	24.3	1809.0	16.4
KHC1_11	2.914	1.70%	0.11828	0.92%	*0.40*	1902.1	27.9	1930.3	16.5
KHC1_12	2.586	1.60%	0.13027	0.92%	*0.40*	2107.6	28.7	2101.6	16.1
KHC1_1	2.874	1.91%	0.12189	0.93%	*0.40*	1924.7	31.7	1984.1	16.5
KHC1_3	3.943	1.88%	0.09062	0.98%	*0.40*	1457.2	24.4	1438.5	18.6
KHC1_22	3.006	2.43%	0.11245	1.11%	*0.40*	1851.4	39.0	1839.4	19.9
KHC1_38	3.138	2.12%	0.11168	1.01%	*0.40*	1783.3	32.9	1826.9	18.2
KHC1_60	5.564	3.51%	0.07452	1.78%	*0.40*	1065.5	34.4	1055.7	35.5
KHC1_52	3.053	1.97%	0.11198	0.97%	*0.40*	1826.5	31.3	1831.9	17.4
KHC1_55	3.013	1.98%	0.11212	0.98%	*0.40*	1847.5	31.7	1834.1	17.7
KHC1_59	3.000	2.04%	0.11696	0.97%	*0.40*	1854.6	32.8	1910.2	17.3

KHC1_76	2.863	1.90%	0.11800	0.95%	*0.40*	1931.2	31.7	1926.2	17.0
KHC1_86	2.998	1.95%	0.12049	0.98%	*0.40*	1855.7	31.4	1963.5	17.3
KHC1_179	2.006	1.41%	0.17528	0.99%	*0.40*	2607.1	30.1	2608.7	16.3
KHC1_164	3.014	1.26%	0.11139	0.99%	*0.40*	1847.1	20.2	1822.2	17.8
KHC1_195	3.058	1.62%	0.11356	1.05%	*0.40*	1823.7	25.7	1857.2	18.8
KHC1_204	2.947	1.42%	0.11183	1.05%	*0.40*	1883.3	23.2	1829.4	19.0
KHC1_273	2.610	1.60%	0.12648	1.04%	*0.40*	2090.7	28.5	2049.6	18.3
KHC1_260	3.001	1.24%	0.11199	0.98%	*0.40*	1853.8	20.0	1832.0	17.6
KHC1_261	2.784	1.80%	0.11798	1.09%	*0.40*	1978.3	30.5	1925.8	19.4
KHC1_240	3.017	1.42%	0.11150	1.02%	*0.40*	1845.5	22.8	1824.0	18.4
KHC1_208	2.995	1.27%	0.11187	0.97%	*0.40*	1857.3	20.4	1830.1	17.5
KHC1_187	2.619	1.30%	0.12817	0.98%	*0.40*	2084.7	23.1	2073.1	17.1
KHC1_180	2.887	1.92%	0.11782	1.03%	*0.40*	1917.1	31.8	1923.4	18.4
KHC1_103	2.873	2.07%	0.11615	1.07%	*0.40*	1925.1	34.3	1897.8	19.1
KHC1_142	1.272	2.13%	0.34951	0.99%	*0.40*	3739.9	60.3	3704.9	15.0
KHC1_136	3.134	2.06%	0.11062	1.06%	*0.40*	1785.1	32.0	1809.6	19.1
KHC1_165	2.876	3.49%	0.11820	1.30%	*0.40*	1923.4	57.9	1929.2	23.2
KHC1_159	3.002	1.98%	0.11384	1.05%	*0.40*	1853.3	31.8	1861.6	18.9
KHC1_128	2.900	1.95%	0.11677	1.04%	*0.40*	1909.6	32.1	1907.4	18.5
KHC1_112	1.967	2.34%	0.16964	1.05%	*0.40*	2649.6	50.6	2554.1	17.4
KHC1_111	3.450	4.56%	0.10940	1.48%	*0.40*	1641.0	65.7	1789.4	26.7
KHC1_100	1.896	2.47%	0.17274	1.04%	*0.40*	2730.2	54.7	2584.4	17.3
KHC1_98	2.959	1.06%	0.11773	0.97%	*0.40*	1876.6	17.3	1922.1	17.3
KHC1_92	3.080	1.25%	0.10991	1.06%	*0.40*	1812.5	19.7	1797.9	19.2
KHC1_80	2.309	1.09%	0.14837	0.98%	*0.39*	2319.4	21.2	2327.3	16.6
KHC1_90	3.000	1.44%	0.11086	1.10%	*0.39*	1854.3	23.2	1813.6	19.8
KHC1_78	3.025	1.80%	0.11228	1.12%	*0.40*	1841.4	28.8	1836.7	20.1
KHC1_82	3.070	1.18%	0.11541	1.01%	*0.34*	1817.9	18.6	1886.3	18.0
KHC1_75	3.274	1.20%	0.10905	1.00%	*0.35*	1718.0	18.1	1783.7	18.1
KHC1_61	3.023	1.86%	0.11168	1.11%	*0.36*	1842.2	29.7	1826.9	20.0
KHC1_46	2.937	1.87%	0.11595	1.15%	*0.36*	1888.9	30.5	1894.6	20.5
KHC1_54	2.321	1.11%	0.17084	0.98%	*0.29*	2309.2	21.5	2565.9	16.2
KHC1_42	2.953	1.19%	0.11952	0.99%	*0.20*	1879.9	19.3	1949.1	17.6

sample name	238U 206Pb	1 sigma % error	207Pb 206Pb	1 sigma % error	*Th U*	206/238 age	1 sigma abs err	207/206 age	1 sigma abs err
< 10 % discordant									
KHC3_633	3.065	1.35%	0.11179	0.99%	*0.37*	1820.5	21.4	1828.7	17.9
KHC3_833	3.174	2.30%	0.11915	1.44%	*0.37*	1765.4	35.4	1943.4	25.4
KHC3_741	2.018	0.87%	0.17649	0.89%	*0.37*	2594.9	18.5	2620.2	14.8
KHC3_776	3.199	1.01%	0.11216	0.91%	*0.37*	1753.6	15.5	1834.7	16.5
KHC3_814	2.677	1.18%	0.13001	0.96%	*0.40*	2045.8	20.7	2098.1	16.7
KHC3_716	3.120	1.05%	0.11260	1.00%	*0.40*	1792.2	16.5	1841.8	18.0
KHC3_410	3.010	1.08%	0.11195	0.99%	*0.40*	1849.4	17.4	1831.4	17.9
KHC3_466	2.801	0.98%	0.12622	0.93%	*0.40*	1968.0	16.6	2046.0	16.3
KHC3_576	3.024	1.95%	0.11277	1.10%	*0.40*	1841.5	31.2	1844.6	19.7
KHC_640	2.915	1.08%	0.11728	0.99%	*0.40*	1901.4	17.8	1915.2	17.6
KHC_567	2.752	1.36%	0.12603	1.00%	*0.40*	1998.3	23.3	2043.3	17.5
KHC_557	5.543	2.16%	0.07367	1.63%	*0.40*	1069.1	21.2	1032.4	32.7
KHC_453	2.544	1.02%	0.13180	0.94%	*0.40*	2137.4	18.5	2122.1	16.4
KHC_471	3.251	1.56%	0.11182	1.12%	*0.40*	1729.0	23.7	1829.2	20.1
KHC_396	1.899	1.18%	0.18833	0.92%	*0.40*	2726.7	26.1	2727.6	15.1
KHC_366	2.685	1.49%	0.12700	1.01%	*0.40*	2041.1	26.0	2056.8	17.7
KHC_325	2.624	0.86%	0.13169	0.90%	*0.40*	2081.7	15.3	2120.6	15.6
KHC_314	1.895	1.83%	0.18421	0.96%	*0.40*	2731.8	40.6	2691.2	15.9
KHC_288	3.068	1.88%	0.11203	0.99%	*0.40*	1818.5	29.7	1832.7	17.9
KHC_255	3.083	1.61%	0.11266	0.94%	*0.40*	1811.2	25.3	1842.7	17.0
KHC_289	3.115	1.82%	0.11321	0.99%	*0.40*	1794.9	28.5	1851.6	17.9
KHC_306	2.947	1.71%	0.11381	0.95%	*0.40*	1883.6	27.9	1861.1	17.0
KHC_279	2.235	1.92%	0.17063	0.94%	*0.40*	2383.5	38.2	2563.8	15.7
KHC_278	5.734	2.60%	0.07352	1.26%	*0.40*	1036.3	24.8	1028.4	25.2
KHC_323	2.596	2.14%	0.12717	1.04%	*0.40*	2100.7	38.2	2059.2	18.3
KHC_400	3.128	2.15%	0.11406	1.12%	*0.40*	1788.3	33.4	1865.0	20.2
KHC_414	2.890	2.26%	0.12349	1.07%	*0.40*	1915.3	37.3	2007.2	18.8
KHC3_472	3.118	2.44%	0.10946	1.05%	*0.40*	1793.5	38.2	1790.4	19.0
KHC3_506	3.525	2.74%	0.09919	1.08%	*0.40*	1610.1	38.9	1608.9	20.0
KHC3_550	2.112	2.35%	0.17553	1.03%	*0.40*	2499.0	48.4	2611.1	17.0
KHC3_645	2.977	2.95%	0.11594	1.10%	*0.40*	1866.9	47.6	1894.5	19.6
KHC3_749	2.680	2.81%	0.12710	1.10%	*0.40*	2044.1	49.0	2058.2	19.3
KHC3_809	3.307	3.28%	0.11265	1.25%	*0.40*	1703.2	48.9	1842.6	22.5
KHC3_779	3.335	2.98%	0.10616	1.10%	*0.40*	1690.6	44.2	1734.5	20.1
KHC3_720	5.902	2.84%	0.07227	1.20%	*0.40*	1008.9	26.5	993.6	24.3

KHC3_739	3.115	2.63%	0.11178	1.08%	*0.40*	1794.8	41.0	1828.6	19.4
KHC3_770	3.294	2.28%	0.10871	0.98%	*0.40*	1709.1	34.1	1778.0	17.7
KHC3_806	2.748	1.67%	0.12791	0.96%	*0.40*	2000.5	28.6	2069.5	16.9
KHC3_821	2.860	1.37%	0.12125	0.91%	*0.40*	1933.2	22.9	1974.6	16.1
KHC3_802	2.005	1.73%	0.18675	0.94%	*0.40*	2608.5	36.9	2713.8	15.5
KHC3_778	2.890	1.55%	0.12012	0.96%	*0.40*	1915.5	25.6	1957.9	17.0
KHC3_677	2.870	1.56%	0.11549	1.01%	*0.40*	1927.2	26.0	1887.6	18.1
KHC3_599	2.084	1.33%	0.17543	0.88%	*0.40*	2526.8	27.7	2610.1	14.6
KHC3_581	3.188	1.52%	0.11352	0.97%	*0.40*	1758.7	23.4	1856.5	17.5
KHC3_556	2.638	1.26%	0.12818	0.91%	*0.40*	2072.1	22.3	2073.1	16.0
KHC3_596	3.010	1.59%	0.11623	0.96%	*0.40*	1849.2	25.5	1899.0	17.1
KHC3_600	2.683	2.14%	0.12772	1.05%	*0.40*	2042.1	37.3	2066.8	18.4
KHC3_643	2.382	2.05%	0.14677	0.97%	*0.40*	2259.3	39.0	2308.6	16.5
KHC3_647	3.106	2.19%	0.11479	1.00%	*0.40*	1799.2	34.3	1876.6	18.0
KHC3_588	2.716	2.27%	0.12908	0.96%	*0.40*	2021.2	39.3	2085.4	16.7
KHC3_628	3.309	2.46%	0.11219	0.98%	*0.40*	1702.1	36.7	1835.2	17.6
KHC3_632	3.296	2.40%	0.11276	0.97%	*0.40*	1708.3	35.9	1844.4	17.5
KHC3_563	2.576	2.54%	0.12905	1.01%	*0.40*	2114.5	45.6	2085.1	17.7
KHC3_530	3.117	3.09%	0.11203	1.12%	*0.40*	1793.9	48.1	1832.7	20.1
KHC3_419	2.260	2.82%	0.16150	0.92%	*0.40*	2361.5	55.5	2471.4	15.4
KHC3_462	3.221	2.94%	0.11117	1.01%	*0.40*	1743.2	44.7	1818.7	18.3
KHC3_497	3.084	2.71%	0.11126	0.93%	*0.40*	1810.4	42.6	1820.1	16.8
KHC3_436	3.142	2.69%	0.11126	0.95%	*0.40*	1781.1	41.8	1820.0	17.1
KHC3_388	3.034	3.02%	0.11714	1.06%	*0.40*	1836.2	48.0	1913.0	18.8
KHC3_324	3.148	2.68%	0.11231	0.95%	*0.40*	1778.2	41.4	1837.2	17.1
KHC3_281	3.090	2.81%	0.11258	0.98%	*0.40*	1807.2	44.1	1841.5	17.7
KHC3_217	3.021	2.83%	0.11342	1.02%	*0.40*	1843.5	45.2	1854.8	18.3
KHC3_192	2.856	2.74%	0.12803	0.93%	*0.40*	1935.2	45.7	2071.1	16.2
KHC3_198	3.010	2.63%	0.11819	0.93%	*0.40*	1849.4	42.2	1929.1	16.5
KHC3_146	2.308	1.43%	0.14609	0.93%	*0.40*	2320.2	27.8	2300.7	15.8
KHC3_125	3.102	1.20%	0.11196	0.90%	*0.40*	1801.4	18.9	1831.4	16.3
KHC3_111	3.295	2.34%	0.11142	1.14%	*0.40*	1708.7	35.1	1822.7	20.5
KHC3_114	2.798	1.37%	0.11709	0.98%	*0.40*	1970.0	23.2	1912.3	17.4
KHC3_130	1.553	1.06%	0.26282	0.87%	*0.40*	3203.9	26.7	3263.7	13.7
KHC3_132	3.153	1.59%	0.11165	1.02%	*0.40*	1775.7	24.7	1826.5	18.4
KHC3_92	2.981	1.79%	0.11639	1.00%	*0.40*	1865.0	29.0	1901.5	17.8
KHC3_26	3.077	1.31%	0.11040	0.94%	*0.40*	1814.2	20.8	1805.9	17.1
KHC3_31	2.944	2.66%	0.11515	1.16%	*0.40*	1884.9	43.4	1882.2	20.8
KHC3_5	2.954	2.54%	0.11106	1.16%	*0.40*	1879.4	41.3	1816.9	20.9
KHC3_259	2.001	2.26%	0.18328	1.02%	*0.40*	2612.9	48.4	2682.8	16.8

KHC3_223	3.137	2.06%	0.11253	1.02%	*0.40*	1783.7	32.0	1840.7	18.4
KHC3_200	3.434	2.38%	0.10889	0.98%	*0.40*	1647.6	34.5	1781.0	17.7
KHC3_147	3.323	2.68%	0.11307	1.20%	*0.40*	1695.8	39.8	1849.4	21.6
KHC3_123	2.991	2.20%	0.11500	1.04%	*0.40*	1859.6	35.5	1879.9	18.6
KHC3_59	2.216	2.53%	0.15532	1.06%	*0.40*	2400.5	50.4	2405.3	17.9
KHC3_42	3.069	4.17%	0.11374	1.41%	*0.40*	1818.3	65.7	1860.0	25.2
KHC3_30	3.213	3.13%	0.11156	1.23%	*0.40*	1746.8	47.7	1825.0	22.1
KHC3_18	2.632	3.42%	0.12797	1.24%	*0.40*	2076.1	60.4	2070.3	21.7
KHC3_73	2.125	2.21%	0.17277	1.04%	*0.40*	2486.2	45.5	2584.7	17.3
KHC3_128b	3.045	2.87%	0.12203	1.22%	*0.40*	1830.4	45.6	1986.1	21.5
KHC3_128a	2.098	5.21%	0.18409	1.00%	*0.40*	2512.2	107.5	2690.1	16.4
KHC3_145b	3.089	5.72%	0.11503	1.35%	*0.40*	1807.9	89.6	1880.3	24.1
KHC3_145a	3.170	5.21%	0.11354	1.12%	*0.40*	1767.6	80.0	1856.9	20.0
KHC3_140	3.134	5.11%	0.11037	1.12%	*0.40*	1785.4	79.2	1805.5	20.2
KHC3_115	1.978	5.01%	0.19091	0.96%	*0.40*	2637.6	107.5	2750.0	15.7
KHC3_136	2.787	4.92%	0.12931	0.94%	*0.40*	1976.5	83.2	2088.6	16.4
KHC3_100	3.114	5.55%	0.11127	1.33%	*0.40*	1795.1	86.4	1820.3	24.0
KHC3_109	2.834	5.22%	0.12630	1.11%	*0.40*	1948.0	87.1	2047.0	19.4
KHC3_80	2.749	5.07%	0.12856	1.07%	*0.40*	2000.3	86.7	2078.3	18.7
KHC3_79	3.076	6.28%	0.11594	1.16%	*0.40*	1814.4	98.6	1894.5	20.6
KHC3_56	5.710	6.36%	0.07214	1.52%	*0.40*	1040.4	60.8	989.8	30.5
KHC3_36	2.919	6.09%	0.12108	0.93%	*0.39*	1899.2	99.4	1972.2	16.5
KHC3_19	2.976	6.08%	0.11907	0.93%	*0.39*	1867.6	97.9	1942.3	16.6
KHC3_69	2.034	6.34%	0.18310	1.00%	*0.40*	2577.5	133.3	2681.1	16.4
KHC3_58	2.228	6.18%	0.17181	0.92%	*0.35*	2389.8	122.2	2575.4	15.3
KHC3_37	2.725	6.18%	0.14080	1.08%	*0.36*	2015.0	106.1	2237.1	18.5
KHC3_15	2.765	6.11%	0.13067	0.91%	*0.20*	1989.8	103.8	2107.1	15.8

sample name	238U 206Pb	1 sigma % error	207Pb 206Pb	1 sigma % error	*Th U*	206/238 age	1 sigma abs err	207/206 age	1 sigma abs err
< 10 % discordant									
PP_31	3.226	3.06%	0.11027	1.44%	*0.40*	1740.8	46.5	1803.8	25.9
PP_30	1.991	1.37%	0.18375	0.93%	*0.40*	2623.0	29.5	2687.0	15.2
PP_29	1.836	1.34%	0.20177	0.95%	*0.40*	2803.1	30.4	2840.5	15.3
PP_28	2.979	1.70%	0.11131	1.09%	*0.40*	1865.9	27.5	1820.9	19.7
PP_27	3.096	1.05%	0.11225	0.95%	*0.40*	1804.4	16.5	1836.2	17.0
PP_26	2.008	0.92%	0.18315	0.89%	*0.40*	2605.1	19.6	2681.6	14.6
PP_25	3.004	0.92%	0.11738	0.95%	*0.40*	1852.3	14.8	1916.7	16.9
PP_24	3.062	1.38%	0.11104	1.01%	*0.40*	1822.0	21.9	1816.5	18.3
PP_23	3.133	0.79%	0.11239	0.92%	*0.40*	1785.6	12.3	1838.3	16.6
PP_22	2.005	1.08%	0.18166	0.90%	*0.40*	2608.5	23.0	2668.1	14.8
PP_21	3.144	1.42%	0.11224	0.98%	*0.40*	1780.1	22.0	1836.0	17.6
PP_20	3.028	1.30%	0.11824	0.96%	*0.40*	1839.7	20.7	1929.8	17.1
PP_19	2.952	1.79%	0.12066	1.06%	*0.40*	1880.7	29.2	1966.0	18.8
PP_18	3.151	1.18%	0.11511	0.97%	*0.40*	1776.7	18.3	1881.5	17.4
PP_17	2.857	2.34%	0.11704	1.12%	*0.40*	1934.9	39.0	1911.5	19.9
PP_16	2.890	1.63%	0.11866	1.00%	*0.40*	1915.7	27.0	1936.1	17.8
PP_15	2.988	2.22%	0.11730	1.14%	*0.40*	1861.2	35.8	1915.4	20.3
PP_14	3.084	1.29%	0.11230	0.94%	*0.40*	1810.7	20.4	1837.0	16.9
PP_13	2.733	1.20%	0.12824	0.94%	*0.40*	2010.3	20.8	2073.9	16.4
PP_12	3.113	1.23%	0.11121	0.94%	*0.40*	1795.9	19.3	1819.2	17.0
PP_11	2.016	1.26%	0.18129	0.91%	*0.40*	2597.1	26.8	2664.7	14.9
PP_10	3.027	1.60%	0.11613	1.03%	*0.39*	1840.2	25.5	1897.5	18.4
PP_9	3.119	1.34%	0.11237	0.98%	*0.39*	1792.8	21.0	1838.0	17.7
PP_8	3.167	1.16%	0.11153	0.93%	*0.40*	1768.9	18.0	1824.6	16.7
PP_7	3.074	2.07%	0.11348	1.11%	*0.34*	1815.8	32.7	1855.9	20.0
PP_6	2.896	1.16%	0.12942	0.89%	*0.35*	1912.3	19.2	2090.2	15.5
PP_5	2.982	1.10%	0.11825	0.91%	*0.36*	1864.5	17.9	1930.0	16.3
PP_4	2.986	1.26%	0.11795	0.95%	*0.36*	1861.9	20.4	1925.4	17.0
PP_3	2.939	1.23%	0.11809	0.95%	*0.29*	1888.0	20.1	1927.6	16.9
PP_2	2.996	1.48%	0.11486	1.02%	*0.20*	1856.8	23.9	1877.7	18.2

APPENDIX D

TERRA-WASSERBERG PLOTS

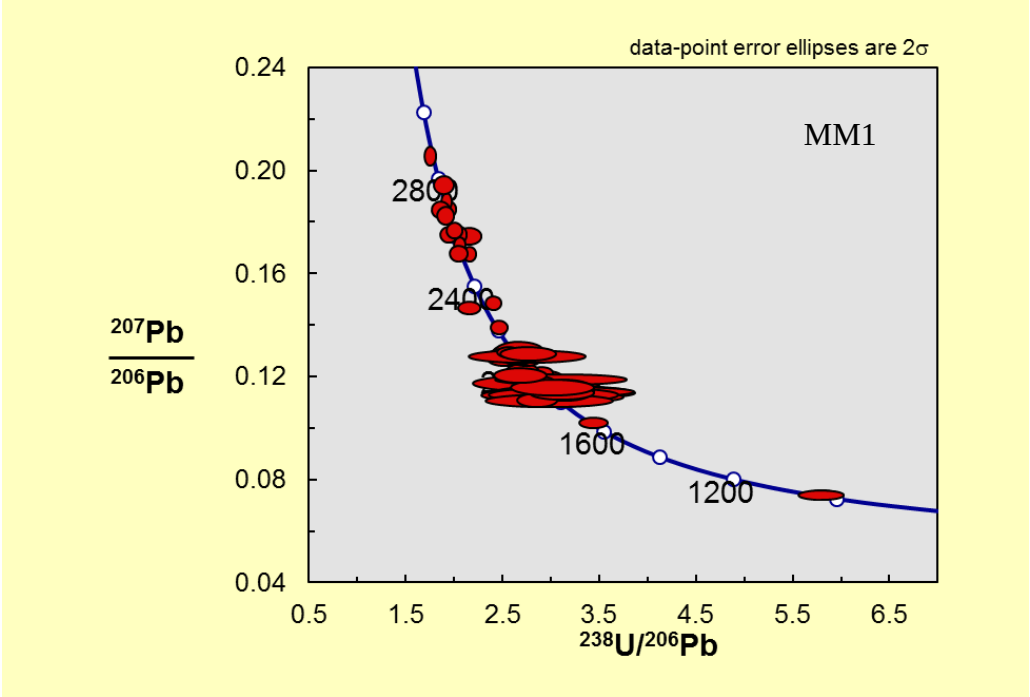

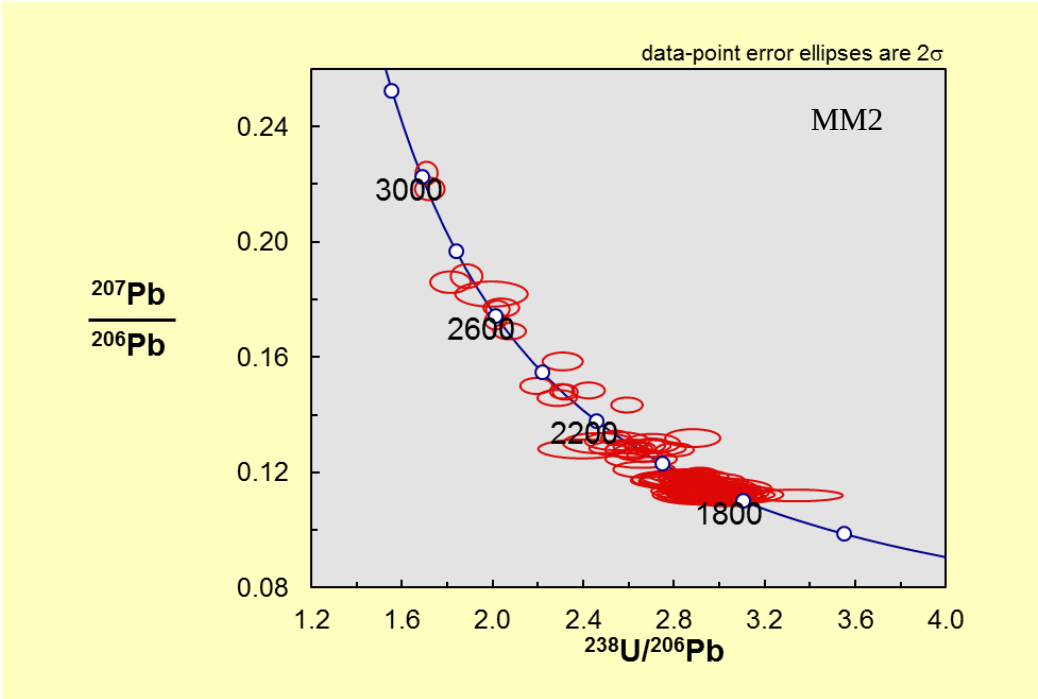

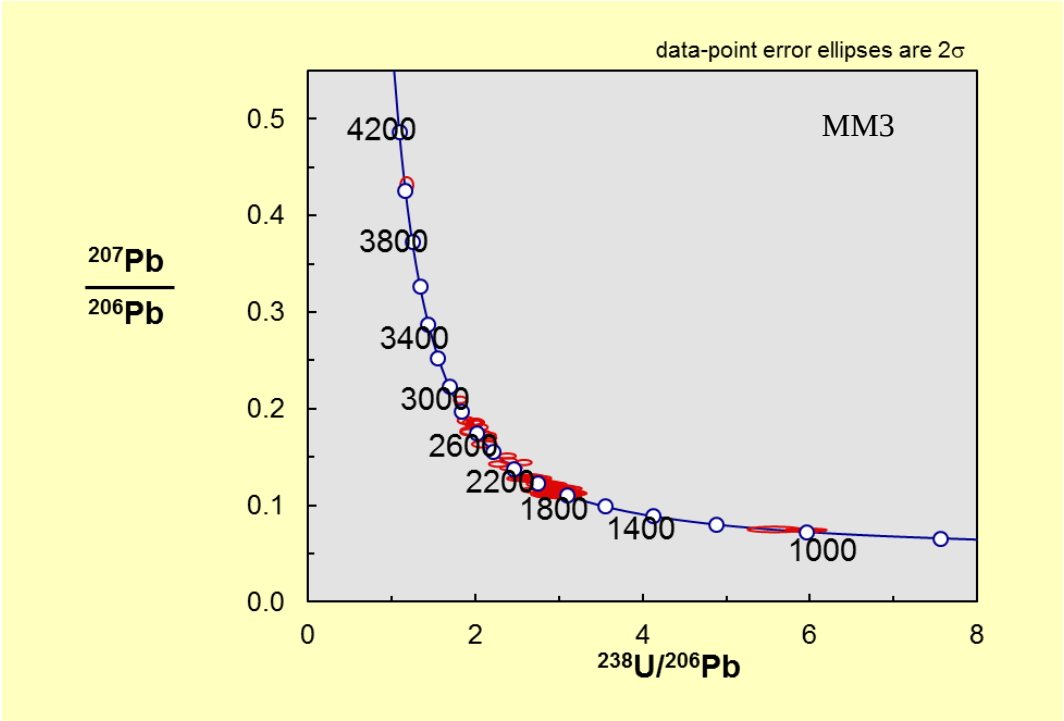
data-point error ellipses are 2σ
MM3
4200
3800
3400
3000
2600
2200
1800
1400
1000
0.5
0.4
0.3
0.2
0.1
0.0
0
2
4
6
8
207Pb/206Pb
238U/206Pb

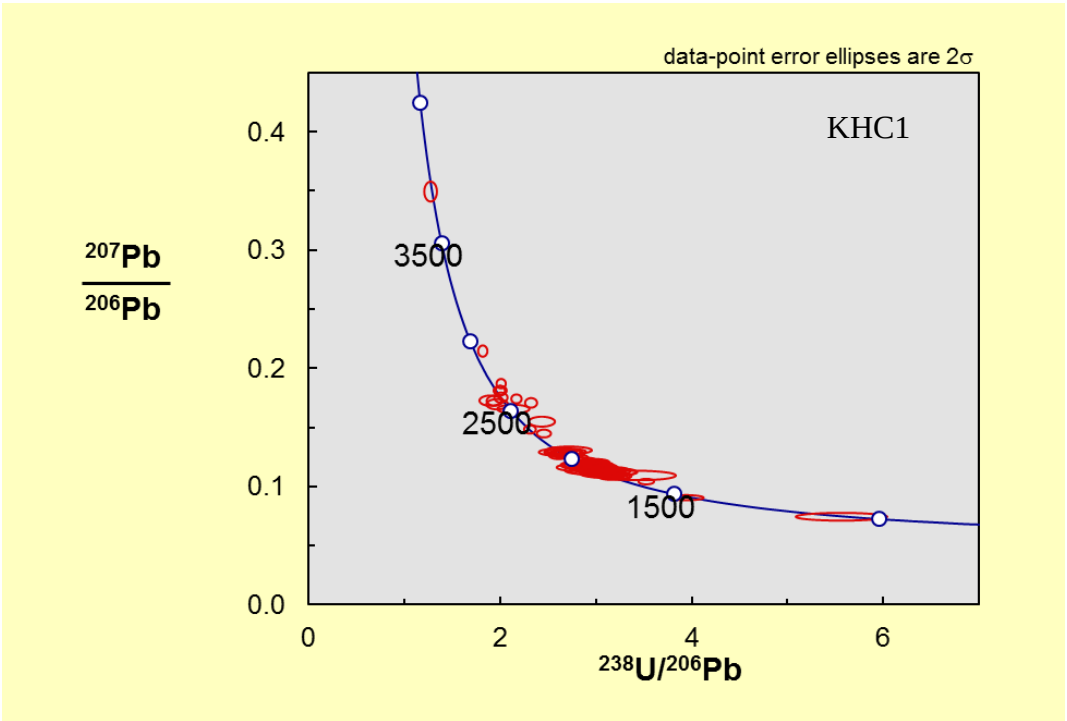
data-point error ellipses are 2σ
KHC1
3500
2500
1500
0.4
0.3
0.2
0.1
0.0
0
2
4
6
207Pb/206Pb
238U/206Pb

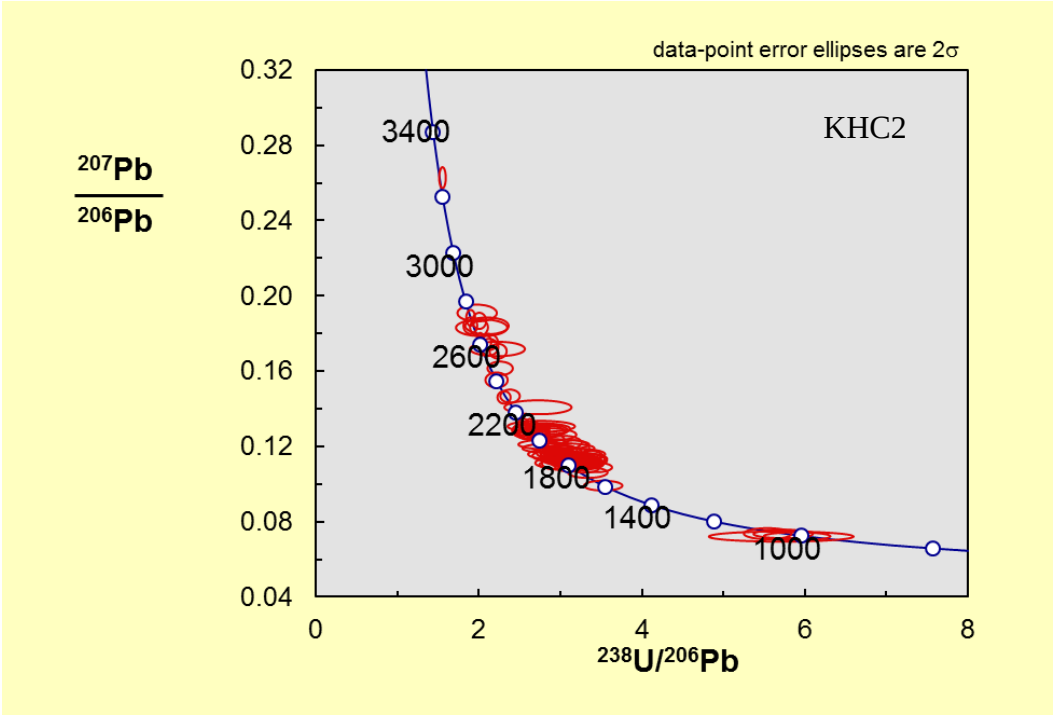
data-point error ellipses are 2σ
KHC2
$^{207}Pb/^{206}Pb$
$^{238}U/^{206}Pb$
0.32
0.28
0.24
0.20
0.16
0.12
0.08
0.04
0
2
4
6
8
3400
3000
2600
2200
1800
1400
1000

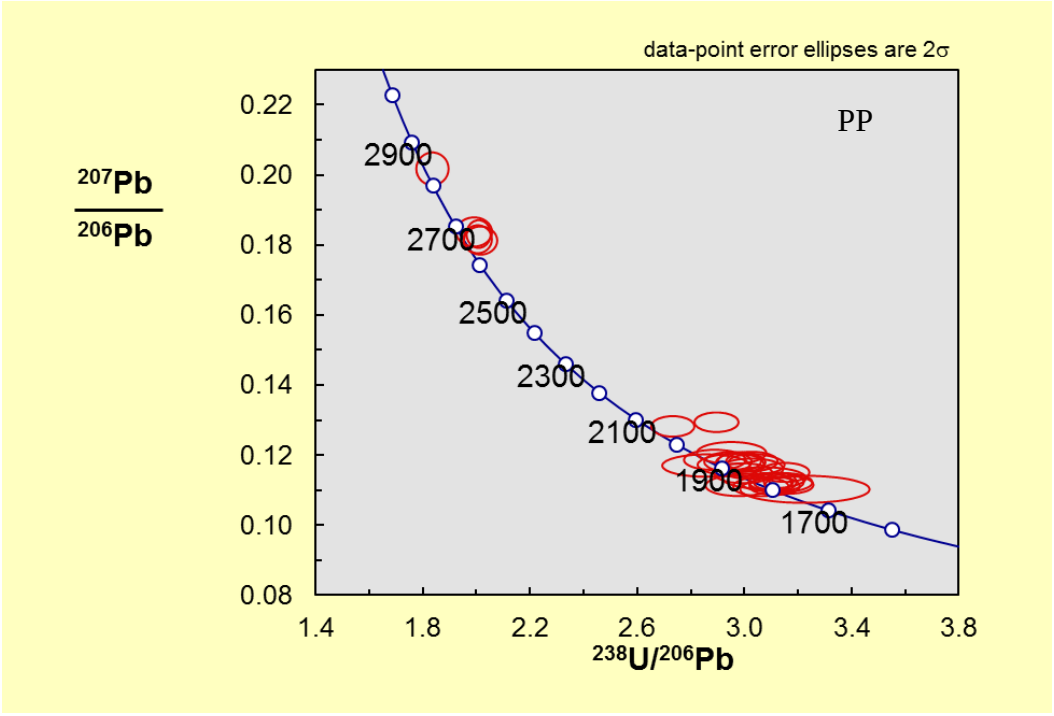
data-point error ellipses are 2σ
PP
$^{207}Pb/^{206}Pb$
$^{238}U/^{206}Pb$
0.22
0.20
0.18
0.16
0.14
0.12
0.10
0.08
1.4
1.8
2.2
2.6
3.0
3.4
3.8
2900
2700
2500
2300
2100
1900
1700

APPENDIX E

CONCORDIA PLOTS

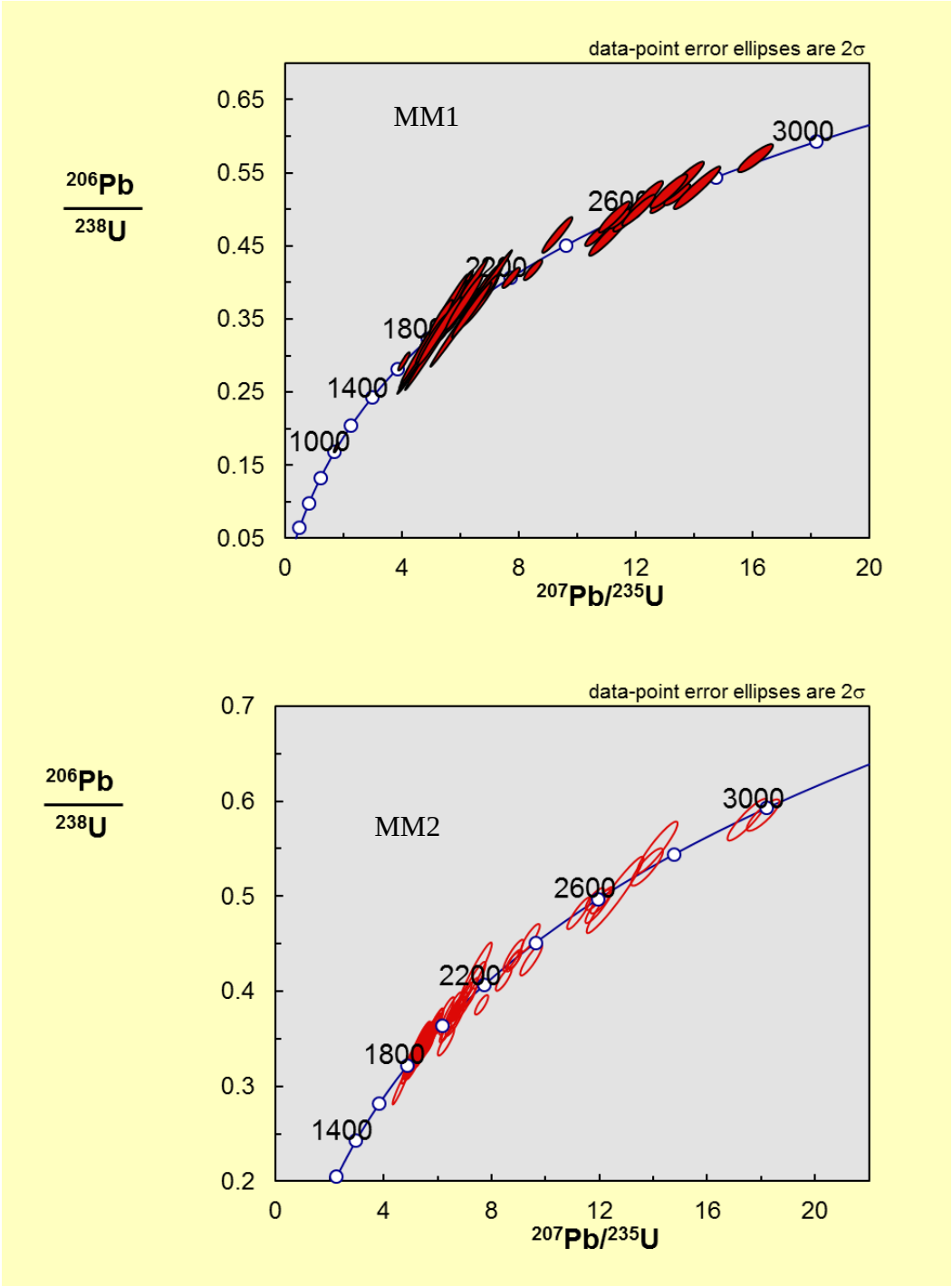

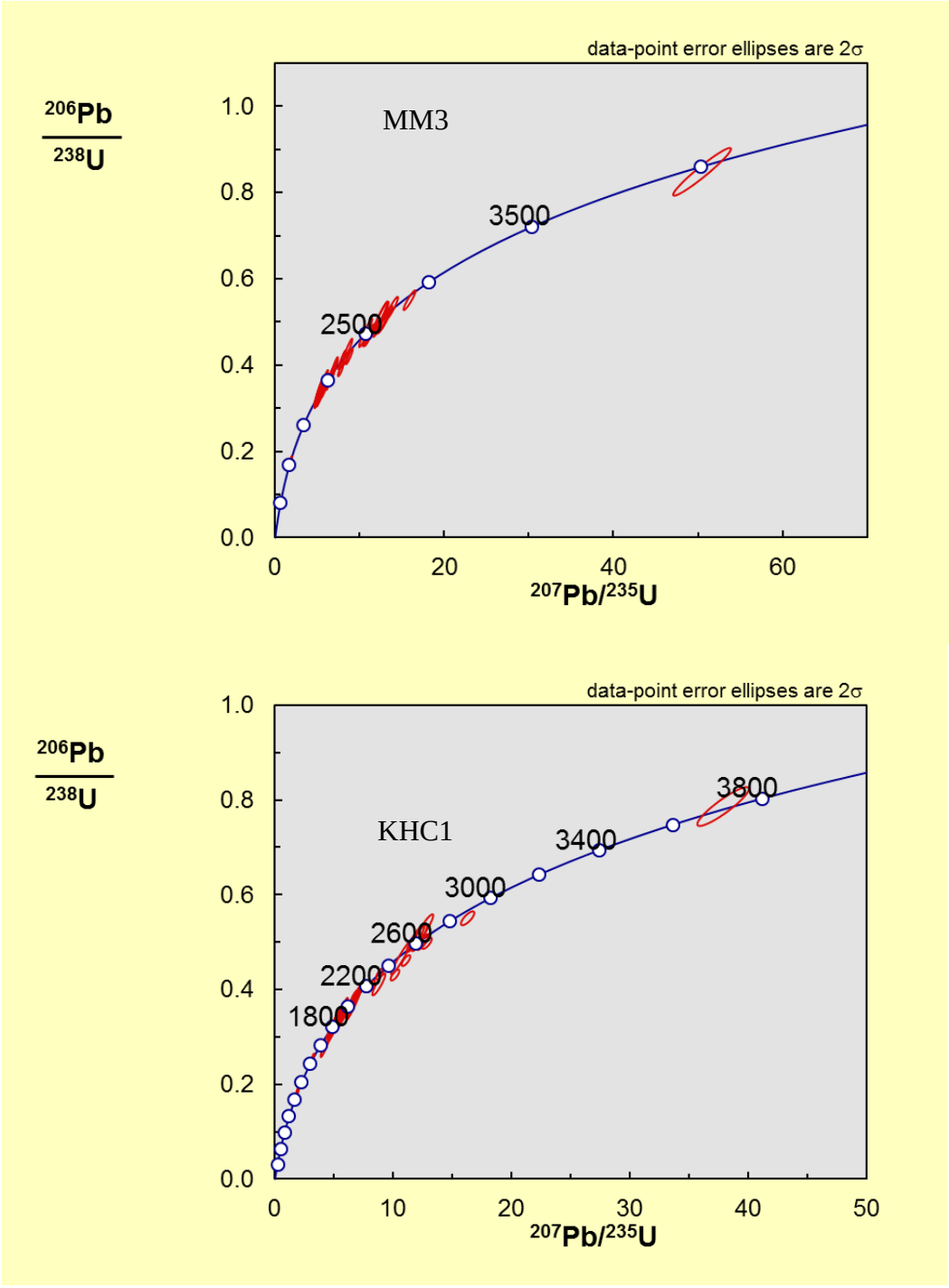
data-point error ellipses are 2σ
206Pb/238U
MM3
3500
2500
1.0
0.8
0.6
0.4
0.2
0.0
0
20
40
60
207Pb/235U
data-point error ellipses are 2σ
206Pb/238U
KHC1
3800
3400
3000
2600
2200
1800
1.0
0.8
0.6
0.4
0.2
0.0
0
10
20
30
40
50
207Pb/235U

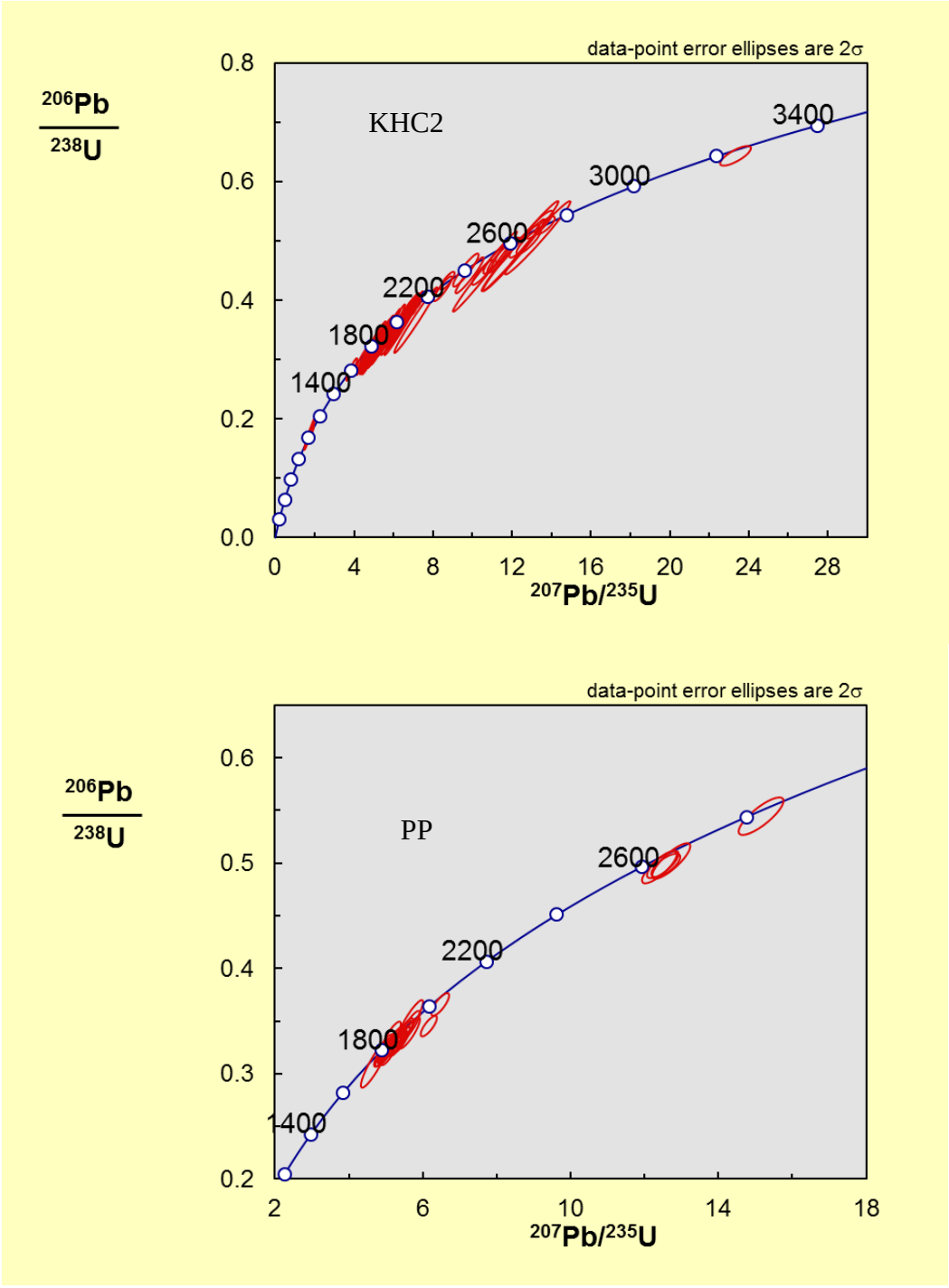
data-point error ellipses are 2σ
$^{206}Pb/^{238}U$
KHC2
3400
3000
2600
2200
1800
1400
0.8
0.6
0.4
0.2
0.0
0
4
8
12
16
20
24
28
$^{207}Pb/^{235}U$
data-point error ellipses are 2σ
$^{206}Pb/^{238}U$
PP
2600
2200
1800
1400
0.6
0.5
0.4
0.3
0.2
2
6
10
14
18
$^{207}Pb/^{235}U$

APPENDIX F

PROBABILITY DENSITY PLOTS

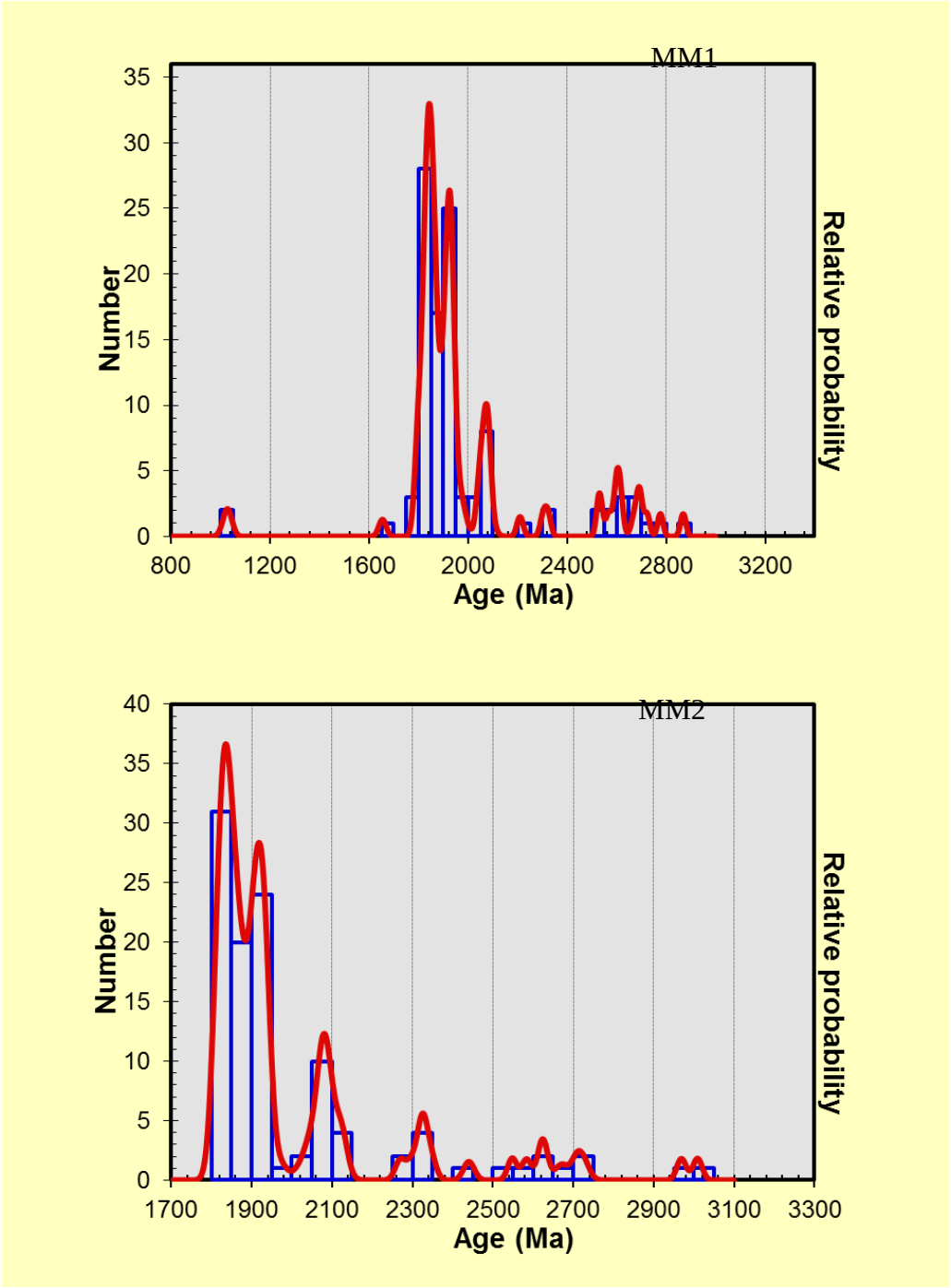

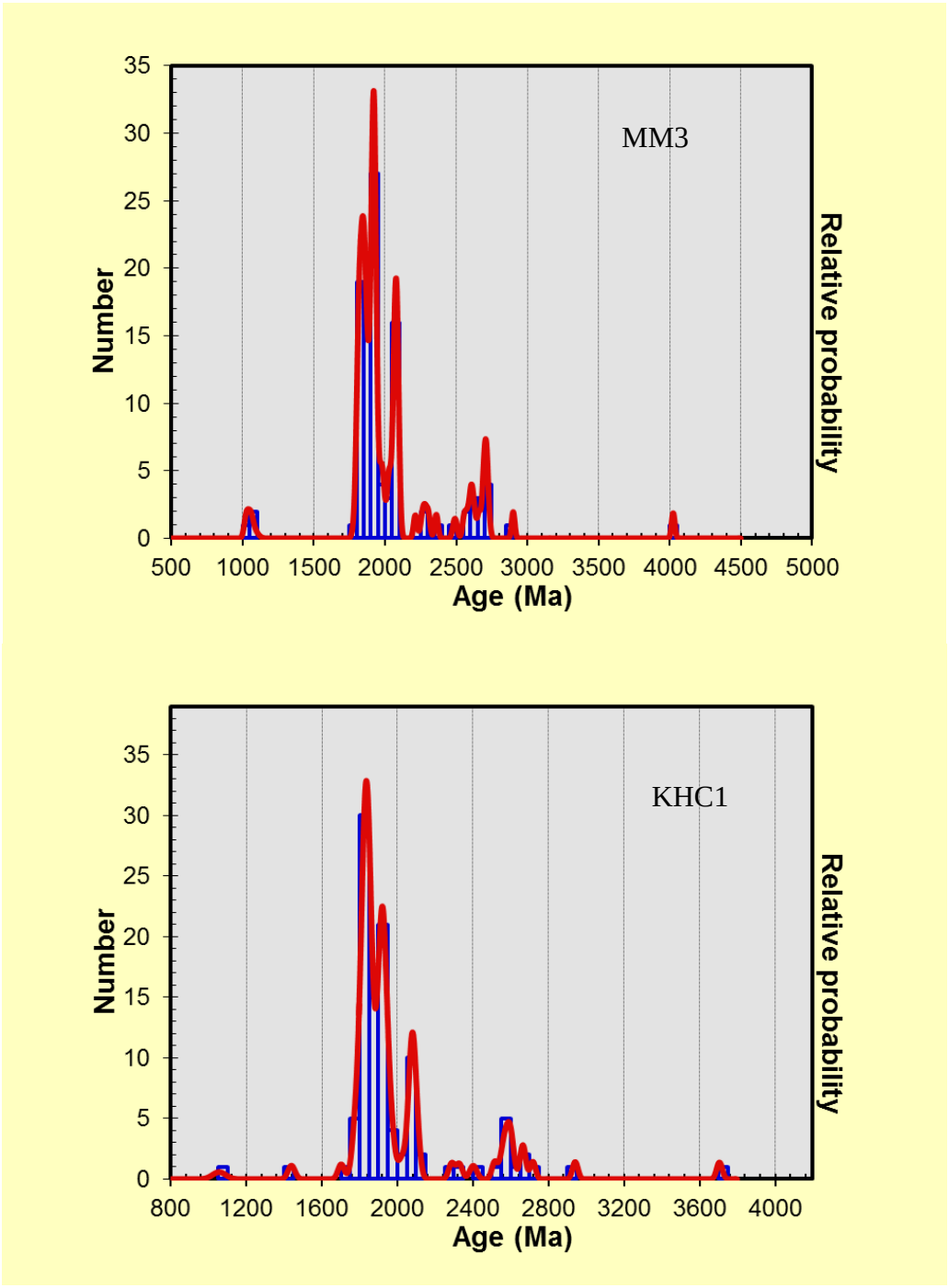
MM3
Number
Relative probability
Age (Ma)
0
5
10
15
20
25
30
35
500
1000
1500
2000
2500
3000
3500
4000
4500
5000
KHC1
Number
Relative probability
Age (Ma)
0
5
10
15
20
25
30
35
800
1200
1600
2000
2400
2800
3200
3600
4000

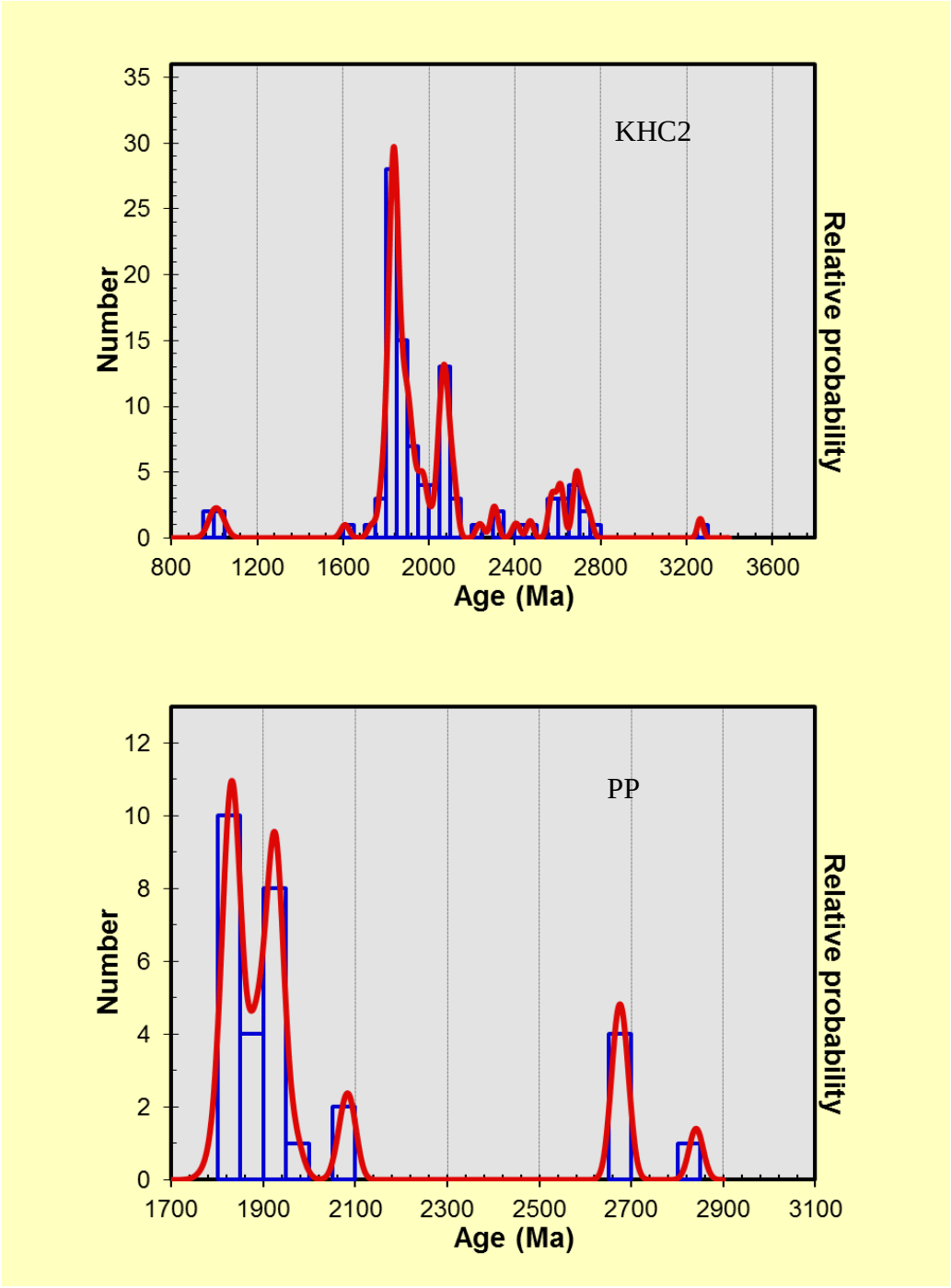
KHC2
Number
Relative probability
Age (Ma)
0
5
10
15
20
25
30
35
800
1200
1600
2000
2400
2800
3200
3600
PP
Number
Relative probability
Age (Ma)
0
2
4
6
8
10
12
1700
1900
2100
2300
2500
2700
2900
3100

VITA

Andrew Paul Hutto received his Bachelor of Science degree in geology from Texas A&M University in College Station, Tx in 2009. He entered the geology program at Texas A&M University in January 2010 and received his Master of Science degree in May 2012. His research interests include clastic sedimentology, sequence stratigraphy, petroleum geology. He plans to pursue a career in the oil and gas exploration industry.

Mr. Hutto may be reached at 9600 Ming Ave. Suite 300 Bakersfield, CA 93309. His email is ahutto87@gmail.com.